Dissertation

On

PERFORMANCE ANALYSIS OF SOLAR AIR HEATER HAVING ARTIFICIAL ROUGHNESS ON THE ABSORBER PLATE

Submitted in partial fulfillment of the requirement for the award of degree of

MASTER OF ENGINEERING

IN

THERMAL

Submitted By

MOHIT SHARMA

Roll No. 801083018

Under the Guidance of

Dr. MADHUP KUMAR MITTAL

Assistant Professor

Mechanical Engineering Department

Thapar University, Patiala

DEPARTMENT OF MECHANICAL ENGINEERING

THAPAR UNIVERSITY

PATIALA-147004, INDIA,

July- 2012

ACKNOWLEDGEMENT

Words are often less to reveals one's deep regards. With an understanding that work like this can never be the outcome of a single person, I take this opportunity to express my profound sense of gratitude and respect to all those who directly or indirectly helped me through the duration of this work.

I take the opportunity to express my heartfelt adulation and gratitude to my supervisor, ***Dr. Madhup Kumar Mittal*** *for their unreserved guidance, constructive suggestions, thought provoking discussions and unabashed inspiration in the nurturing work. It has been a benediction for me to spend many opportune moments under the guidance of the perfectionist at the acme of professionalism. The present work is testimony to their activity, inspiration and ardent personal interest, taken by them during the course of this work in its present form. I am grateful to* ***Dr. Ajay Batish****, Prof. & Head, MED for providing the facilities for the completion of the work. No words acknowledge the support I received from my friends for their valorous help and co-operation.*

I take pride of myself being son of ideal parents for their everlasting desire, sacrifice, affectionate blessings, and help, without which it would not have been possible for me to complete my studies.

I would like to thank to all the members and employees of Mechanical Engineering Department, Thapar University Patiala for their everlasting support. Above all, I express my indebtedness to the "ALMIGHTY" for all His blessing and kindness.

Mohit Sharma

Registration No.: 801083018

DECLARATION

I hereby declare that the thesis entitled **"PERFORMANCE ANALYSIS OF SOLAR AIR HEATER HAVING ARTIFICIAL ROUGHNESS ON ABSORBER PLATE"** is an authentic record of my study carried out as requirement for the award of degree of **Master of Engineering (Thermal)** at **Thapar University, Patiala** under the guidance of **Dr.MADHUP KUMAR MITTAL**, Assistant Professor, Department of Mechanical Engineering, Thapar University, Patiala. The matter embodied in this report has not been submitted in part or full to any other university or institute for the award of any other degree.

(Mohit Sharma)
Reg. No. 801083018

This is to certify that above declaration made by the student concerned is correct to the best of my knowledge & belief.

(DR. MADHUP KUMAR MITTAL)
Assistant professor
Mechanical engineering Department
Thapar University, Patiala

Countersigned by:

Dr. AJAY BATISH
Professor and Head,
Mechanical Engineering Department,
Thapar University,
Patiala-147004

Dr. S.K. MOHAPATRA
Dean of Academic Affairs,
Thapar University,
Patiala-147004

ABSTRACT

The thermal performance of solar air heater is generally poor due to low heat transfer coefficient between the absorber plate and air flowing in the duct. In order to improve the thermal performance artificial roughness is provided on the underside of absorber plate due to which turbulence is created in the heat transfer zone and ultimately performance of solar air heater improves considerably. Present work aimed at analyzing the performance of solar air heater in terms of effective efficiency by providing different types of artificial roughness on the absorber plate. The effective efficiency has been computed by using the correlations for friction factor and heat transfer developed by various investigators for different roughness elements. Under the present study effective efficiency in the lower range of Reynolds's number is found to be maximum for solar air heater roughened with Dimple shaped ribs and in the higher range of Reynolds's number Arc shaped wires resulted in better effective efficiency. It is also found under the present study that effective efficiency attains a maximum value for dimple shaped ribs of approx. 0.8236 at Reynolds's no. of 12000 for relative roughness height of 0.034. In present work FEM simulation software, ANSYS version 12(workbench mode) has been used for simulation. Fluid flow (FLUENT) module has been used in present work. Fluid flow (FLUENT) module predicts the outlet temperature, velocity, flow behavior to great accuracy due to application of thermal loading on the work piece. Different types of thermal loading that can be applied on the work piece in Fluid flow (FLUENT) module are temperature, convection, radiation and heat flux. Using the Fluid flow (FLUENT) module of ANSYS heat transfer analysis was conducted on the solar air heater provided with different types of artificial roughness on the absorber plate. Simulation predicts the temperature distribution, velocity distribution and flow behavior of air flowing inside the duct. Simulation showing a little variation in results as obtained from numerical analyses which are quite acceptable. Solar air heater provided with Grooved shaped ribs gives maximum enhancement in outlet temperature of air as temperature changes from 27°C to 67°C in that case.

LIST OF FIGURES

LIST OF TABLES

NOMENCLATURE

D	Equivalent diameter of air channel(m)
p	Roughness pitch
e	Height of Reynolds element(m)
e/D	Relative roughness height
p/e	Relative roughness pitch
e^+	Roughness Reynolds number
Re	Reynolds number
l/s	Relative length of grit
l/e	Relative long way length of mesh
g	Groove distance from rib centre line(m)
g/p	Relative groove position
H	Height of duct(m)
H/D	Duct aspect ratio
Nu	Nusselt number
A_C	Element area(m^2)
F'	Collector efficiency factor
V	Velocity of air in duct(m/s)
L	Collector length(m)
P	Mechanical power
q_u	Useful thermal gain
h	Heat transfer coefficient
U_L	Overall loss coefficient
f	Friction factor
I	Radiation intensity

Greek letters

η_{th}	Thermal efficiency
ρ	Density(kg/m^3)
ΔP	Pressure drop (N/m^2)
η_{eff}	Effective efficiency
ϕ	Chamfer angle(^{0})

CONTENTS

CHAPTER 1

INTRODUCTION

1.1 INTRODUCTION

As we all know for the economic & industrialization development of the whole world, energy plays an important role in that regard. There are many sources conventional & non conventional from where we met our energy demands but with the rate at which our fossil fuels are depleting it is necessary to shift focus on non conventional sources of energy which meets the energy demands for the generation to come. It becomes necessary to give emphasis on sustainable energy which reduces the consumption of fossil fuels to great extent.

Nowadays the major area of interest of researchers is to make solar energy as the primary source of energy. Studies have also shown that solar energy has vast potential to meet world's energy demand as it exceeds 8000 times by world's energy demand.

Out of many non-conventional sources of energy, solar energy is one which has the tendency to meet world energy demands for many years. Solar energy have many advantages like cheapest source of energy, inexhaustible and non polluting source of fuel and above all these advantages one of the most important advantage which a solar energy possess is its availability. It is estimated that amount of solar energy reaching the earth's surface is many times more than rate of energy consumption by all energy consuming devices put together.

When there is advantages of anything some limitations are also associated with it and solar energy in this regard have no exception. The major limitation of solar energy is its intensity and its fluctuating nature. Solar radiation rarely exceeds $1kw/m^2$ even in earth's hottest region. But in spite of all these limitation solar energy is the most promising non conventional source of energy which meets energy demand in nearby future to large extent.

Solar energy have wide range of application like water heating, air heating, power generation, solar furnace, photo-voltaic cells, solar refrigeration, photo chemical and photo biological conversion & so on.

1.2 SOLAR COLLECTOR

Solar collector is a device which acts like a heat exchanger which converts solar energy that falls on its absorber plate into thermal energy and later this thermal energy is used to raise the temperature of the fluid flowing inside the collector. The fluid may be air or water. In order to achieve different temperature ranges for working fluid the collector may be of different shape and design. Solar air heater is the most widely used solar energy collection device due to its simplicity, minimal use of material and cost. Solar air heater is widely used for application related to moderate application like curing of industrial products, space heating, seasoning of timber, crop drying and drying of clay building components.

1.3 WORKING PRINCIPLE OF SOLAR COLLECTOR

Solar collector is generally a flat box and has three main parts, i.e. transparent cover, tubes for carrying working fluid and an insulated back plate. Solar collector works on the green house effect principle; solar radiation incident upon transparent surface of solar collector and transmitted through though this surface as a result of which heat energy is trapped inside the solar collector because solar collector is evacuated from inside and this trapped heat energy is used to heat the working fluid. Insulation is provided to avoid heat losses.

1.4 FLAT PLATE COLLECTOR[17]

Flat plate collector which are of non concentrating type are most convenient when temperature below 90°C are required for applications like space heating, service water heating. In flat plate collector there is no provision for sun tracking due to its fixed position. Flat plate collector facing south in the northern hemisphere and facing north in the southern hemisphere. The optimum tilt angle of the collector is equal to the latitude of the location with variation of 10-15°. They are made in rectangular panels from about 1.7 to 2.9 sq m in area and are simple to construct. Flat plate collector can absorb both direct and diffuse radiation. Flat plate collector is shown in figure 1.1.

Figure 1.1 Flat Plate Collector[17]

The majority of flat plate collector main five components

- The transparent cover which may consist of one or more sheet of glass.
- Tubes, fins, channels are integral with the collector absorber plate which carry the water, fluid or air.
- The absorber plate normally metallic.
- Insulation should be provided at both sides to prevent heat losses.
- The casing which encloses the absorber & other components.

Depending upon the type of working fluid being used, flat plate collector may be classified as solar liquid heater and solar air heater

1.4.1 Solar Liquid Heater

Solar liquid heater is a flat plate and tube type collector as shown in figure 1.2. It consists of a flat surface with high absorptivity for solar radiation called the absorbing surface. Typically a metal plate usually of copper, aluminium with tubing of copper in thermal contact with the plate is the most commonly used materials.

The absorber plate is made from a sheet metal of 1 to 2 mm in thickness while the tubes which are also made of metal and their diameter ranges from 1 to 1.5 cm. They are brazed, clamped to

the bottom of absorber plate with pitch ranging from 5 to 15 cm. The thermal insulation of 5 to 10 cm is placed behind the absorber plate to prevent the heat losses from the surface. The insulation material like mineral fiber and glass wool are used. The front cover is mostly glass which is transparent to incoming radiation and opaque to infra red radiation. The liquid heated is generally water however in some cases, mixture of water and ethylene glycol is used.

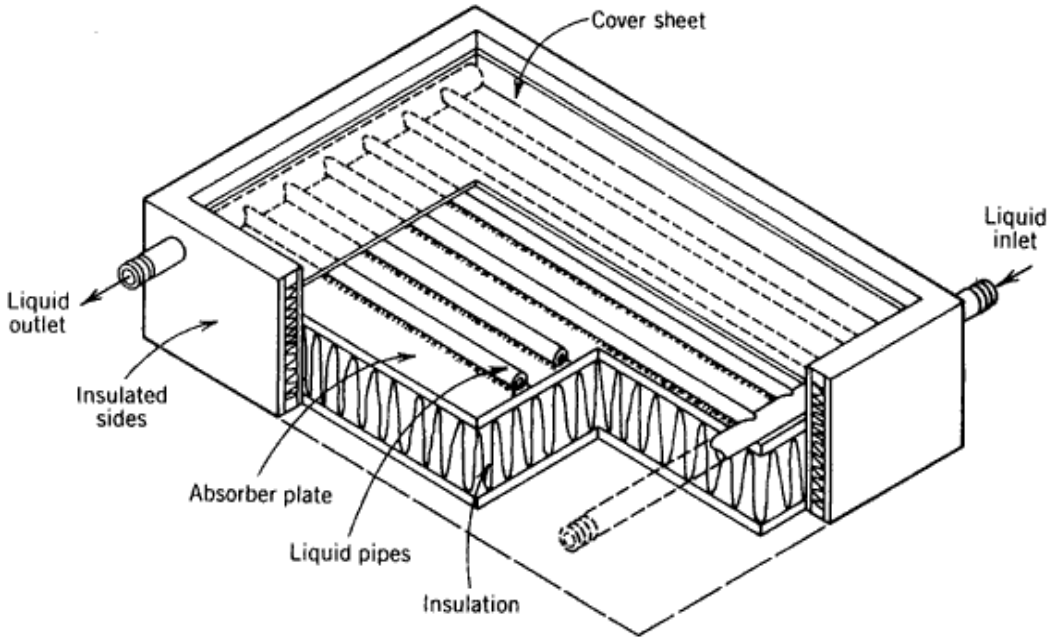

Figure 1.2 Solar Liquid Heater[17]

1.4.2 Solar Air Heater

Solar air heater as shown in figure 1.3 heat air directly as there is no heat transferring medium. Solar air heaters are of two types: Glazed and Unglazed.

In glazed solar air heater there is a transparent top sheet and also insulated side and bottom surface to minimize heat losses. In glazed solar air heater air flow above or below the absorber plate and scrubbing heat from the absorber plate. It is used for applications such as space heating and drying while in unglazed solar air heater there is no provision for transparent cover and air flow directly above or below the absorber plate. It is used for application like pre heating of makeup air in commercial buildings.

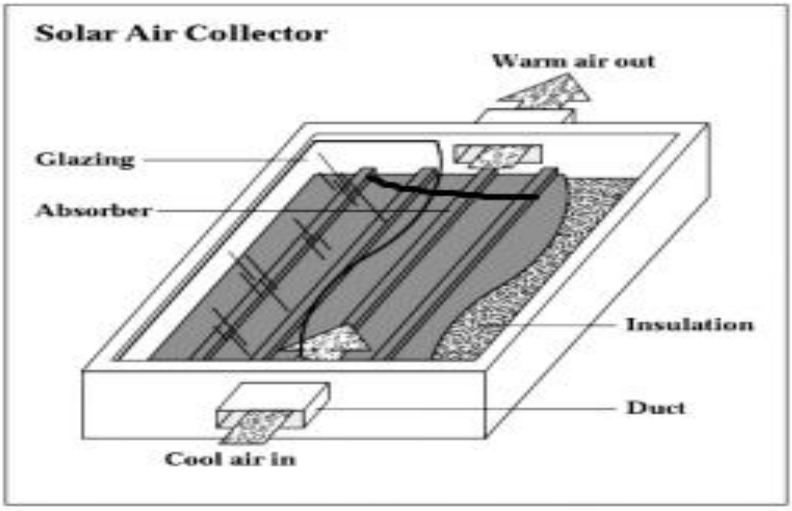

Figure 1.3 Solar Air Heater[17]

Air has been used so far to a lesser extent as the heat transport medium in solar collector but it may have some advantage over water.

- In case of solar air heater no other heat transfer medium is required as in case of liquid solar heater.
- In case of solar air heater the material used for the collector and duct is light because the pressure of air at inlet is atmospheric.
- Overall operating load on collector is less because air is lighter than water.
- If there is any leakage in case of solar air heater it does not cause any serious problem except there is some heat loss.

1.4.2.1 Solar Air Heater with Smooth Absorber Surface

In solar air heater provided with smooth absorber surface there is no hindrance in the path of flowing air and there is a formation of laminar sub layer in the heat transfer zone as a result of which heat transfer capability between the absorber plate and flowing air is low and ultimately it results in decrease of thermal efficiency. Performance of air heater can be improved

- By adding fin to increase the heat transfer area.
- Roughening of the rear part of plate to promote turbulence & improve the convective heat transfer coefficient.

1.4.2.2 Solar Air Heater with Artificially Roughened Absorber Surface

In order to increase the thermal efficiency of solar air heater breaking of laminar sub layer which form in the heat transfer zone is necessary so that turbulence is created in this zone and finally heat transfer coefficient increases.

Breaking of laminar sub layer is possible by providing artificial roughness underneath the absorber plate as a result of which heat transfer area increases. Roughness is created on the absorber plate by providing ribs underneath the absorber plate. Ribs are of various types like V shaped ribs, wedge shaped ribs, angled circular ribs and square ribs. Ribs no doubt increase the turbulence but on the other hand it also increases the pumping power required to force the air into the heater. Therefore turbulence is created only in the laminar sub layer and it is decided by shape and arrangement of roughness element.

1.5 FACTORS AFFECTING THE PERFORMANCE OF SOLAR COLLECTOR[17]

There are several factors which affects the thermal performance of solar air heater namely glazing material, insulation, air flow configuration, absorber plate material, collector tilt angle, surface coating.

1 Glazing

Heat losses through the glass plate due to convection and radiation can be minimized by providing glazing due to which layers of stagnant air is formed and it reduces the convective heat loss to a great extent. Therefore glazing acts like a barrier against heat loss and the double glazing is the optimum no. of glazing used for most of the application. The glazing material should be such that it has high transmissivity to incident solar radiation and low transmittance to the radiation emitted by the absorber plate. Low iron tempered glass &PMMA acrylic glass are the most commonly used glazing material. Glazing also prevents the solar collector from dust, snow, rain etc. glazing material should posses the following properties

- Lightweight
- High Strength
- Ability to withstand the damage caused by solar radiation & other environmental components

2 Insulation

In order to reduce the heat losses through the edges and from the bottom surface insulation must be provided. Insulation minimized the heat losses and finally increases thermal efficiency. The desirable properties for insulation material are

- Low thermal conductivity
- Low density
- Long life & low cost
- Ability to withstand shrinkage, deterioration when exposed to high stagnation temperature of around 200c.

Most commonly used insulation materials are glass wool and fiberglass but it should be free from binding agents which decomposes at higher temperature. The insulation should at least thermal resistivity of $0.57W/m^20C$ & thickness should be 5 cm to 8 cm.

3 Air Flow Configuration

There are various types of air flow configuration like air flow at the top, bottom and both top and bottom of absorber plate. It was observed that when mass flow rate is small multi air flow gave good results and when mass flow rate is large bottom flow gave good result provided that emissivity of both base and absorber plate is low but if the emissivity is high both arrangement gives somewhat same performance. It was also observed that when air flow at the top of absorber plate it increases the heat losses to large extent

Aspect ratio which is the ratio of channel depth to its length also affects the air flow configuration performance and due to this there should be some optimum value of aspect ratio because if aspect ratio is large it decreases the top losses but also decreases the convective heat transfer coefficient. Similarly if aspect ratio is small convective heat transfer coefficient increases but also top heat losses increases.

4 Absorber Plate Material

Absorber plate is the surface on which solar radiation incident and its material also affects the Performance of solar collector most commonly used plate material is copper, steel, aluminium. The table 1.1 shows the characteristics of different plate materials.

Table 1.1 Characteristics of Different Plate Materials[17]

Item	Specific Gravity ($lb/in^{3)}$	Thermal Conductivity	Plate Thickness(in)	Weight per square foot (lb)
Copper	0.82	226	0.016	1
Aluminium	0.10	122	0.032	0.6
Steel	0.28	27	0.064	3.9

5 Collector Tilt Angle

The factor which influence the performance of solar collector is its inclination from the horizontal plane because that angle decides how much solar radiation collected per unit area. It was observed that when collector oriented in such a way that it faces to the north in southern hemisphere at that time it collects maximum solar radiation without any solar tracking. The optimum angle is that angle at which collector exposed to solar radiation most of the time during the day and it is obtained by inclined the solar collector normal to the sun's incident angle. As the position of sun vary throughout the day and year it is very difficult to change the angle throughout the day. Therefore optimum angle should be calculated for a season instead for a day.

6 Surface coating

Absorber plate surface should be such that it reflects least amount of solar radiation incident on it for this purpose coating is done on absorber plate. The material used for coating must have high absorptivity & low emissivity but it is difficult to obtain such material therefore surface coating of black chrome which has 0.95 absorptivity and 0.62 emissivity is used. The thickness of coating also affects the performance of solar collector. Generally surface coating of black chrome of thickness 0.15 mm is applied.

1.6 GAP IN LITERATURE

A lot of work has been done in the field of solar air heater. Few researchers have worked on the different roughness geometries to enhance the efficiency of solar air heater. Still there is large scope of work in this field. Sufficient work has not been done to predict the performance of solar air heater provided with artificial roughness. No work has been done to predict the performance (in terms of effective efficiency) by varying the relative roughness height (e/D), comparison of performance of different roughness geometries, CFD based performance analysis of artificially roughened solar air heater.

1.7 OBJECTIVES OF PRESENT WORK

- To analyse the performance (in terms of effective efficiency) of artificially roughened solar duct by varying the relative roughness height.
- To compare the performance of different roughness geometries.
- CFD based performance analysis of artificially roughened solar duct.
- To compare the results obtained from mathematical modelling & CFD analysis.

1.8 ORGANIZATION OF THESIS

Chapter1 covers brief introduction to solar collector, working principle of solar collector, types of solar collector, factor affecting the performance of solar collector.

Chapter 2 presents the extensive literature review of research work which has been done by different researchers in the past .This literature is divided into five categories: Concept of artificial roughness, Flow pattern, Roughness geometries used in solar air heater ducts, Thermal efficiency of solar air heater, Effective efficiency of solar air heater.

Chapter 3 covers problem formulation for the thesis work. It presents the simulation methodology and mathematical modelling to be adopted.

Chapter 4 covers the mathematical modelling results for artificially roughened solar air heater. It also includes the simulation results for solar air heater provided with different type of roughnesses on its absorber plate.

Chapter 5 covers the conclusion regarding results obtained for various artificially roughened solar air heaters. It also includes the future scope of work and references.

CHAPTER 2

LITERATURE REVIEW

2.1 REVIEW OF LITERATURE

In this chapter, an extensive review of literature in the area of solar energy collection system, with special reference to artificial roughness on absorber plate is being presented. It has been brought out that there are several schemes that can be implemented to enhance the thermal performance of this most commonly employed energy collection devices. These methods along with their enhancement potential have been discussed in this chapter.

2.2 CATEGORIZATION OF LITERATURE

Literature is divided into following categories:

1 Concept of artificial roughness
2 Flow pattern
3 Roughness geometries used in solar air heater ducts
4 Thermal efficiency of solar air heater
5 Effective efficiency of solar air heater

2.2.1 Concept of Artificial Roughness

The thermal efficiency of solar air heater is generally poor due to low heat transfer co-efficient between the absorber plate and the air flowing in to the duct due to the formation of laminar sub layer on the absorber plate which acts as heat transferring surface.

Therefore, in order to increase the heat transfer co-efficient and thermal efficiency various methods have been employed in which there is a provision for various design flow arrangement. There are generally two methods by which breaking of laminar sub layer is possible so that turbulence is created in the heat transfer zone & finally heat transfer co-efficient increases to a large extent.

Out of these two methods the first method is providing porous packing inside the duct it provides high heat transfer area, energy absorption in depth and finally turbulence is increased which is essential condition for increasing heat transfer co-efficient between the absorber plate and the flowing air in the duct. This method is suitable for increasing the thermal performance of conventional solar heater.

The other method for improving the heat transfer co-efficient is providing artificial roughness below the absorber plate so that turbulence is created in the laminar sub layer. Therefore, artificial roughness increases the heat transfer area which is essential condition for improving heat transfer coefficient. The solar air heater is considered to be a rectangular channel with one rough surface and three smooth surfaces therefore roughness is provided only on the surface on which solar energy incident. The easiest method of providing artificial roughness on absorber plate is having ribs on the absorber plate.

Ribs are of various types like V-shaped ribs, wedge shaped ribs, angled circular ribs. Ribs no doubt increase the heat transfer co-efficient by increasing turbulence in the laminar sub-layer but due to this increase in turbulence friction layer in the duct will occur. Therefore more pumping power is required to overcome these friction losses so that air will propel in the duct smoothly and easily. It is found from many investigations that in solar air heater the Reynolds's number ranges from 2000<Re<15000.therefore it becomes necessary that turbulence is created only in the laminar sub layer so that heat transfer increases with minimum pumping power required. Therefore it becomes very necessary that thermal hydraulic performance have been investigated for various roughness elements so that it gives an idea about optimum artificial roughness design which gives maximum heat transfer between the absorber plate and the air flowing in to the duct with minimum power requirement to force the air in to duct. It is necessary that turbulence is created only in the laminar sub layer and this is possible only when height of roughness element is small in comparison to duct. There are several parameter which decide the shape and arrangement of roughness element, first is roughness element have height (e) and the pitch (p). There is a dimensionless parameter (e/D) that is relative roughness height D is equivalent diameter of the air passage (m) and relative roughness (p/e) which decides the roughness

arrangement. Square ribs are mostly used but chamfered, circular, semi circular and grooved section have been studied to get the most beneficial arrangement.

2.2.2 Flow Pattern

The geometry of the artificial roughness can be of different shapes and orientations. Flow patterns were discussed with respect to different types of artificial roughness elements as below.

2.2.2.1 Effect of Rib

The most important effect produced by the presence of a rib on the flow pattern, was the generation of two flow separation regions, one on each side of the rib. The vortices so generated are responsible for the turbulence and hence the enhancement in heat transfers as well as in the friction losses takes place.

2.2.2.2 Effect of Rib Height and Pitch

Prasad and Saini (1988) show the flow pattern downstream of a rib as the rib height and pitch were changed. Due to flow separation downstream of a rib, reattachment of the shear layer does not occur for a pitch ratio of less than about 8. Maximum heat transfer has been found to occur in the vicinity of a reattachment point. It is reasonable to accept that a similar effect can be produced by decreasing the relative roughness pitch (p/e) for a fixed relative roughness height (e/D). For relative roughness pitch considerably less than about 8, the reattachment will not occur at all resulting in the decrease of heat transfer enhancement. However, an increase in pitch beyond about10 also results in decreasing the enhancement. It can therefore be concluded that there occurs an optimum combination of pitch and height that will result in maximum enhancement.

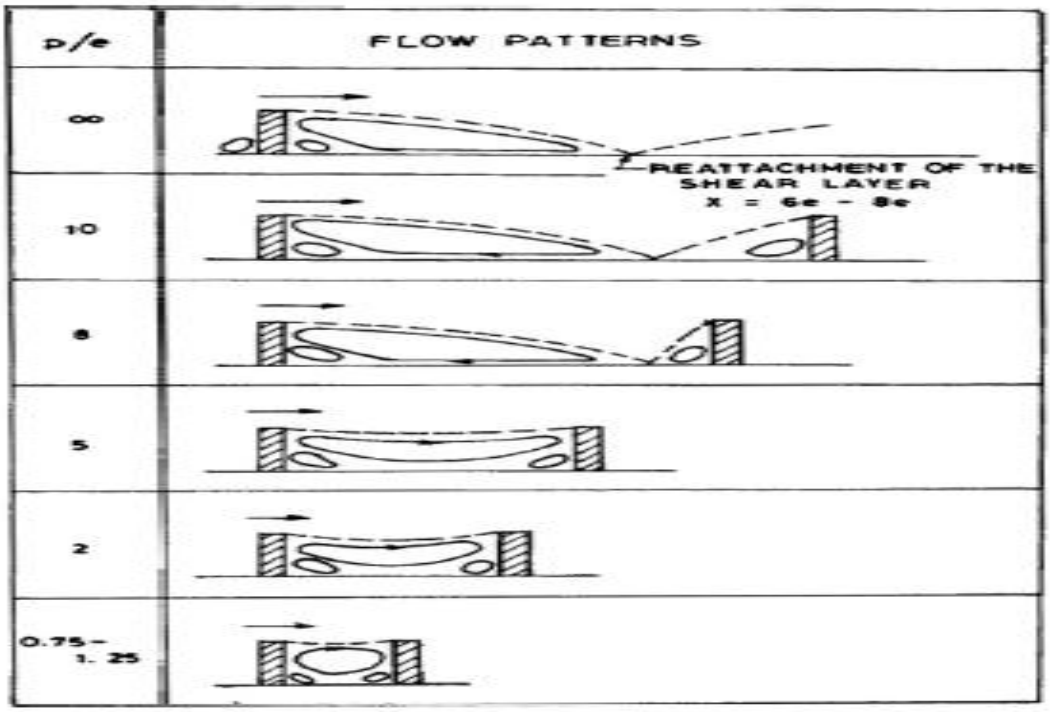

Figure 2.1 Flow Pattern Downstream the Roughness as a Function of Relative Roughness Pitch[23]

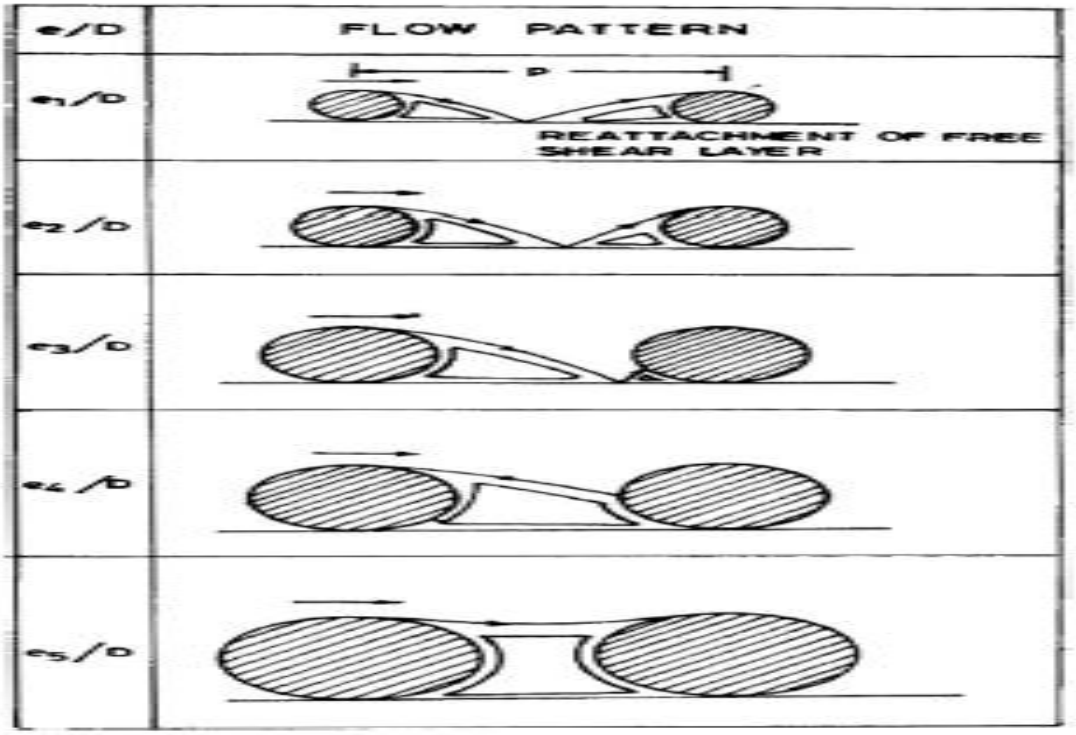

Figure 2.2 Flow Pattern the Roughness as a Function of Relative Roughness Height[23]

2.2.2.3 Effect of Inclination of Rib

Apart from the effect of rib height and pitch, the parameter that has been found to be most influential is the angle of attack of the flow with respect to the rib position i.e.skewness of rib towards the flow. Span wise counter rotating secondary flows created by angling of the rib, appear to be responsible for the significant span wise variation of heat transfer coefficient. It was pointed out that whereas the two fluid vortices immediately upstream and downstream of a transverse rib were essentially stagnant relative to the mainstream flow which raises the local fluid temperature in the vortices and wall temperature near the rib resulting in low heat transfer. The vortices in the case of angled ribs move along the rib so subsequently join the main stream, the fluid entering near the leading end of rib and coming out near the trailing end. These moving vortices therefore bring in cooler channel fluid in contact with leading end raising heat transfer rate while the trailing end heat transfer is relatively lower. This phenomenon therefore results in strong span wise variation of heat transfer.

2.2.2.4 Effect of V-Shaping of Rib

The possibility of further enhancing the wall heat transfer by the use of V-shaped ribs was based on the observation of the creation of secondary flow cell due to angling of the rib resulting in a region of higher heat transfer near the leading end. By splitting the long angled rib into a V - shape to form two leading ends and a single trailing end (apex of V), a much larger (about double) region of high heat transfer was produced. It was infect the formation of two secondary flows cells instead of one as in the case of transverse rib that results in higher overall heat transfer in the case of V-shaped ribs.

2.2.3 Roughness Geometries Used in Solar Air Heater Ducts [23]

In order to increase the heat transfer co-efficient the roughness element have to be considered only on that wall which receive the solar radiation whereas remaining three walls remain un affected from solar radiation due to this consider solar air heater as a rectangular duct with one rough surface and remaining three surface as smooth. The flow pattern and heat transfer characteristic are completely different in this case as from duct with two opposite rough surface. There are different types of roughness element geometries which were investigated by various investigators.

1 Small Diameter Wire

Prasad and Saini (1988) investigated heat transfer and friction factor varies with relative roughness height (e/D) & relative roughness pitch (p/e). It has been found from investigation that as the relative roughness height increases rate of heat transfer decreases whereas rate of friction factor increases. Whereas the relative roughness pitch increases both heat transfer and friction factor decreases. It has been found that Nusselt number and friction factor increased maximum up to 2.38 and 4.5 times when compared with the smooth duct. According to Webb &Eckert (1972) the optimal thermo hydraulic performance could be achieved at e+ of 24. The type and orientation of geometry is shown below in figure 2.3.

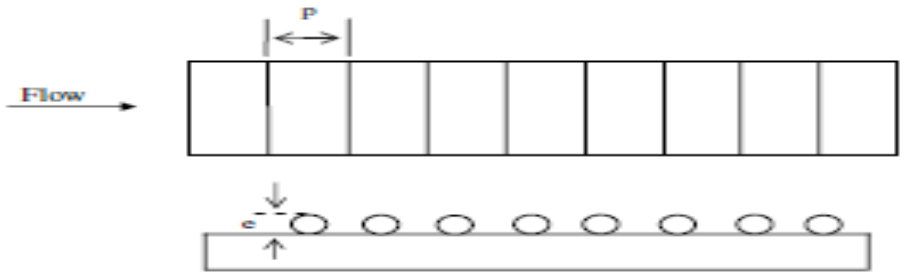

Figure 2.3 Orientation of Small Diameter Wire[23]

Gupta et al (1983) investigated that heat transfer and friction influenced by the roughness height, angle of attack and Reynolds number for the circular wire ribs. It has been found that heat transfer and friction factor increases up to 1.8 and 2.7 times when compared to smooth duct and it has also been investigated that when angle of attack become 60 degree and 70 degree than it led to maximum heat transfer and friction factors. It has also been investigated that the optimum thermo hydraulic performance for roughness surface corresponds to relative roughness height of 0.033 & Reynolds number around 14000. The orientation of the geometry is shown below in figure 2.4.

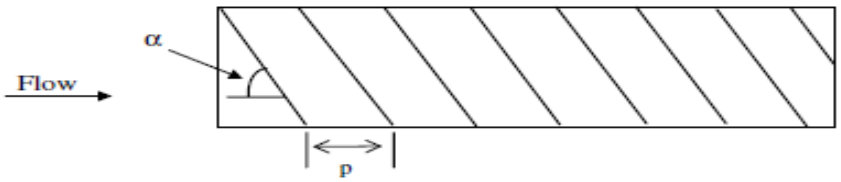

Figure 2.4 Orientation of Circular Wire [23]

Verma and Prasad (2000) also investigated the effect of above parameter on heat transfer and friction factor for circular ribs and it has been found that when the roughness Reynolds number e+ was 24 then it corresponds to optimal thermo hydraulic performance which would be around 71%.

2 Expanded Material

Saini and Saini (1997) investigated expanded wire mesh as a roughened element and it has been observed that heat transfer and friction factor varies with relative long way length of mesh (l/e) and relative short way length of mesh (l/s). The expanded wire mesh geometry is shown below in figure 2.5

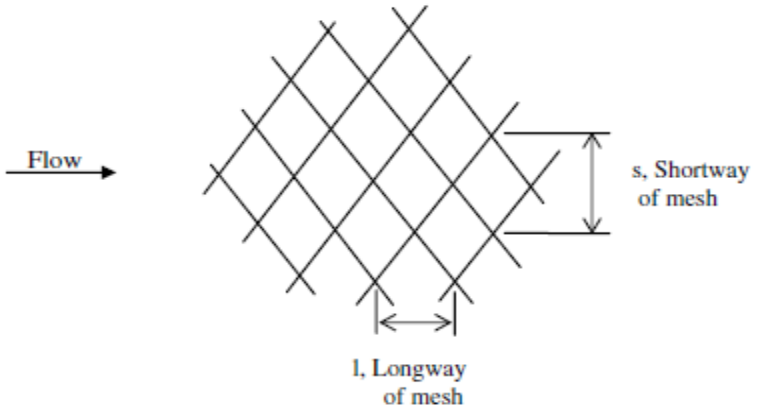

Figure 2.5 Orientation of Expanded Metal Mesh [23]

It has been found that maximum Nusselt number and friction factor obtained when relative long way length of mesh was 46.87 and 71.87 respectively and similarly for short way length of mesh the maximum Nusselt number and friction factor were obtained as 25 and 15 respectively.

3 V-Shaped Ribs

Muluwork et.al (1988) investigated the effect of v-shaped ribs on thermal performance of roughened solar air heater. There was one dimensionless parameter known as relative groove position (g/p) which was considered to compare different configurations. It has been found that Stanton number increases with relative roughness length ratio. It has also been observed that Stanton number for v-down discrete ribs was higher than v-up discrete ribs. The orientation of geometry is shown below in figure 2.6.

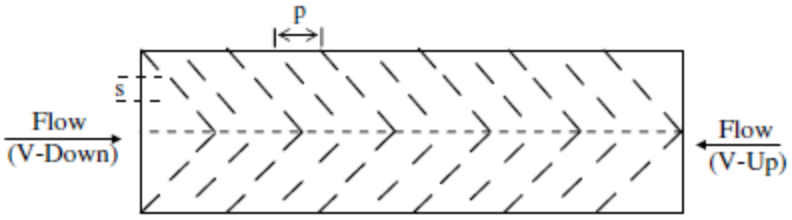

Figure 2.6 Orientation of V Shaped Discrete Ribs [23]

Momin et. al (2002) investigated the effect of v-shaped ribs on heat transfer and fluid flow characteristics. The geometry under investigation is shown in figure. In this investigation Reynolds number ranges from 2500-18000, relative roughness height ranges from 0.02 -0.034 and angle of attack ranges from 30-90° and relative pitch was fixed of 10. It has been observed that both friction factor and Nusselt number increases with Reynolds number but increase of Nusselt number was less as compared to friction factor. It has been found that when angle of attack was 60 degree and relative roughness height of 0.034 then corresponding to this values the Nusselt number increases 1.14 times as compared to inclined ribs and 2.30 times increases when compared with smooth plates. The orientation of geometry is shown below in figure 2.7.

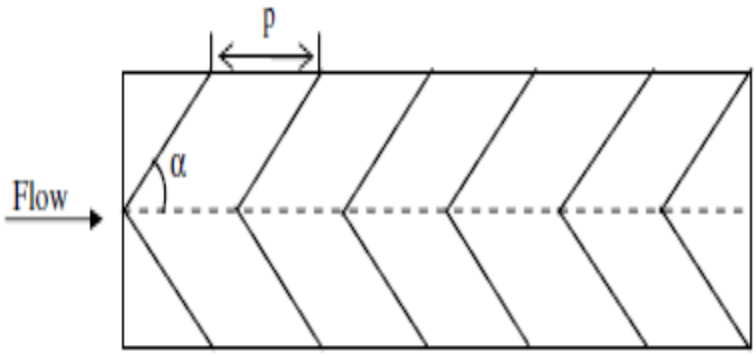

Figure 2.7 Orientation of V Shaped Ribs[15]

4 Chamfered Ribs

Karwa et. al (1988) observed the effect of rib head chamfer angle (ϕ) and duct aspect ratio (H/D) ratio on heat transfer and friction factor for rectangular duct provided with integral chamfered ribs as roughness element. The geometry used is shown below in figure 2.8.

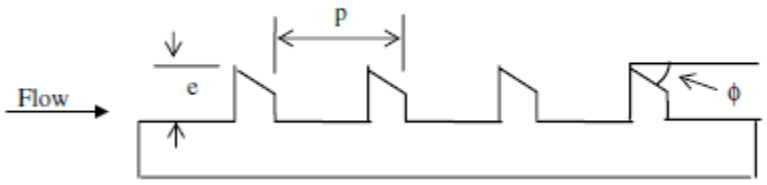

Figure 2.8 Orientation of Integral Chamfered Ribs [9]

The presence of chamfered ribs increases the Stanton number up to 2-3 times when compared with smooth duct. It has been found that when the chamfer angle was 15° then maximum heat transfer and friction factor occurs and also when aspect ratio increases from 4.65-9.66 the heat transfer first increases and after that it attains a constant value and when this value increases from 4.65-7.75 the friction factor decreases and attains a constant value.

5 Wedge Shaped Ribs

Bhagoria (2002) used the wedge shaped ribs as a roughness element and investigated the effect of relative roughness pitch, relative roughness height and wedge angle on heat transfer and friction factor respectively. The geometry used is shown below in figure 2.9.

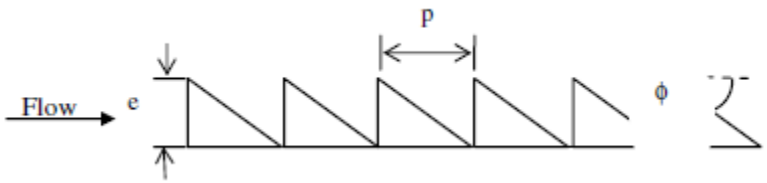

Figure 2.9 Orientation of wedge Shaped Ribs [23]

It has been found that when wedge shaped ribs were used the Nusselt number increases up to 2.4 times and friction factor increases up to 5.3 times when compared with the smooth duct . It has

also been found that maximum heat transfer occurs when wedge angle is 10° and relative roughness pitch was around 7.57.

Sahu & Bhagoria (2005) performed experiment and investigated the effect of broken transverse ribs which was used as a roughness element and it has been found that when value of relative roughness pitch was 20 then it corresponds to maximum value of Nusselt number. From the experiment it was concluded that maximum thermal efficiency was to be the order of (51-83.5%) for roughened solar air heater.

6 Combination of Different Roughness Element

Jaurker (2006) performed experiment and investigated the effect of rib grooved on one broad wall of solar air heater on heat transfer and friction characteristics. In this experiment it has been observed that maximum heat transfer occurs when relative roughness pitch was about 6 and also when groove position to pitch ratio was 0.4 then it corresponds to optimum condition for heat transfer. The geometry used is shown below in figure 2.10.

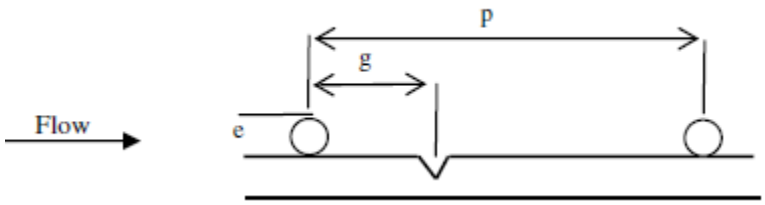

Figure 2.10 Orientation of Grooved Ribs[7]

7 Chamfered Rib Groove

Layek et al. (2007) performed experiment on chamfered rib groove which act as an artificial roughness for solar air heater and investigated the dependency of heat transfer and friction factor on relative roughness pitch, chamfer angle, relative groove position and relative roughness height. The geometry used is shown below in figure 2.11.

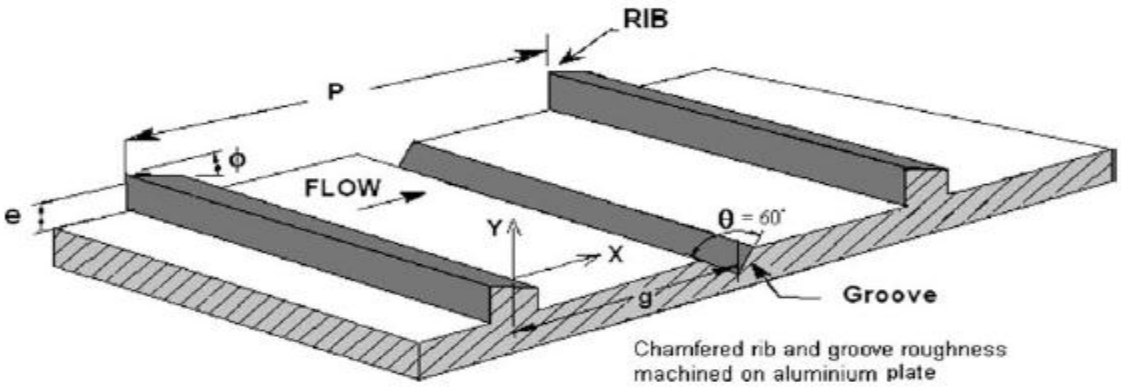

Figure 2.11 Orientation of Chamfered Grooved Ribs[11]

The results obtained after conducting an experiment were

- Nusselt number & friction factor increased by 3.24 & 3.78 times respectively as compared to smooth surface.
- Relative roughness pitch of 6 & relative groove position of 0.4 corresponds to maximum heat transfer.
- Nusselt number attains a maximum value at chamfer angle of 18° but friction factor increases slowly with chamfer angle.

8 Dimple Shaped Roughness

Saini and Verma (2008) used the dimple shaped roughness geometry and investigated the variation of heat transfer and friction factor w.r.t relative roughness height and relative roughness pitch. It was found that by providing dimple shaped roughness there was a considerable increase in heat transfer. Nusselt number had its maximum value at relative roughness height of 0.0379 and relative roughness pitch of 10 and friction factor had its minimum value at relative roughness height of 0.0289 and relative roughness pitch of 10. The geometry used is shown below in figure 2.12.

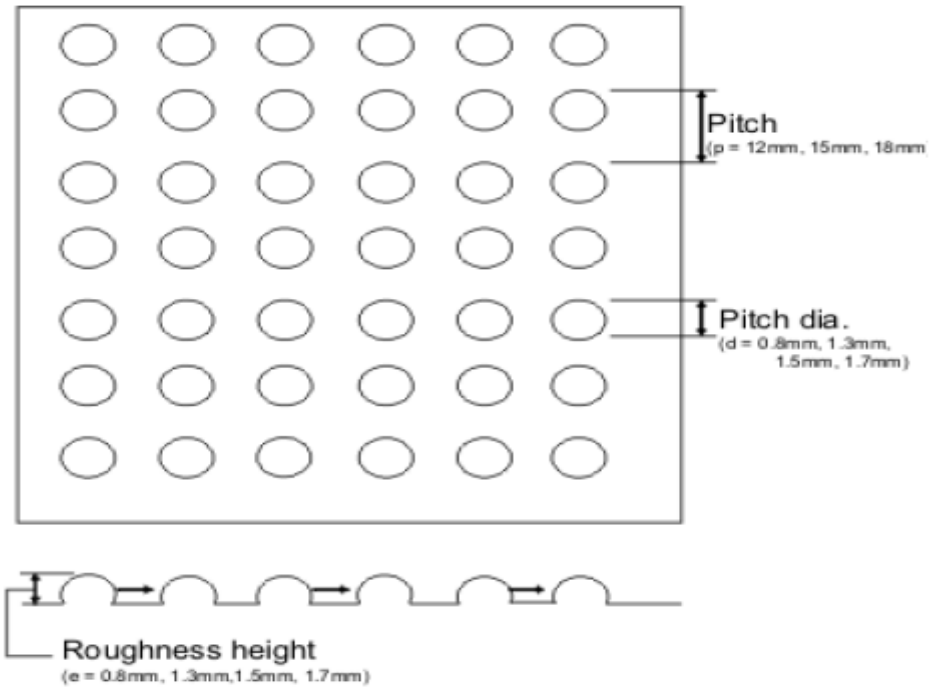

Figure 2.12 Orientation of Dimple Shaped Roughness[19]

9 Metal Grit Ribs

Karmare and Tikekar (2007) performed experiment on solar collector having metal grit ribs as the roughness element & studied the effect of relative roughness pitch (p/e), relative roughness height (e/D), relative length of grit (l/s) on heat transfer and friction factor. The geometry used is shown below in figure 2.13.

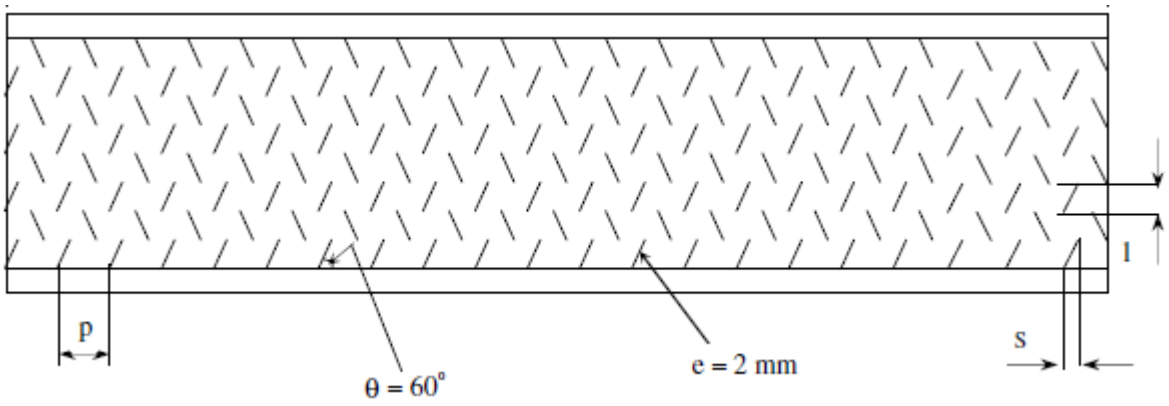

Figure 2.13 Orientation of Metal Grit Ribs[8]

The results obtained after conducting an experiment were

- Nusselt number and friction factor increases up to 2 and 3 times respectively when compared to smooth surface.
- Heat transfer had its maximum value at e/D =0.044, l/s = 1.72, p/e = 17.5 and friction factor had its maximum value at e/D = 0.044, l/s = 1.72, p/e = 12.5
- Optimum performance was found for e/D = 0.044, l/s = 1.72, p/e = 17.5

10 Inverted U Shaped Turbulators

Bopche and Tandale(2009) performed experiment by using inverted U shaped turbulators as the roughness element and it was found that even at relatively low Reynolds number (Re<5000) there was a considerable increase in heat transfer . The geometry used is shown below in figure 2.14.

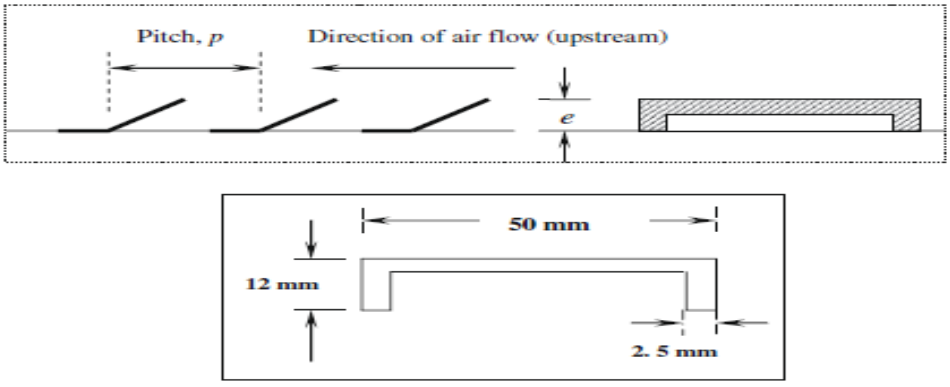

Figure 2.14 Orientation of Inverted U Shaped Turbulators[2]

The results obtained after conducting an experiment were:

- Maximum increase in friction factor and Nusselt number values were of the order of 2.50 and 2.388.
- When compared with smooth duct maximum increase in friction factor and Nusselt number values were of the order of 3.72 and 2.82.

11 Arc Shape Ribs

Saini and Saini (2008) performed experiment by using arc shaped ribs as the roughness element and studied the effect of angle of attack (α/90) and relative roughness height (e/D) on heat transfer and friction factor. The geometry used is shown below in figure 2.15.

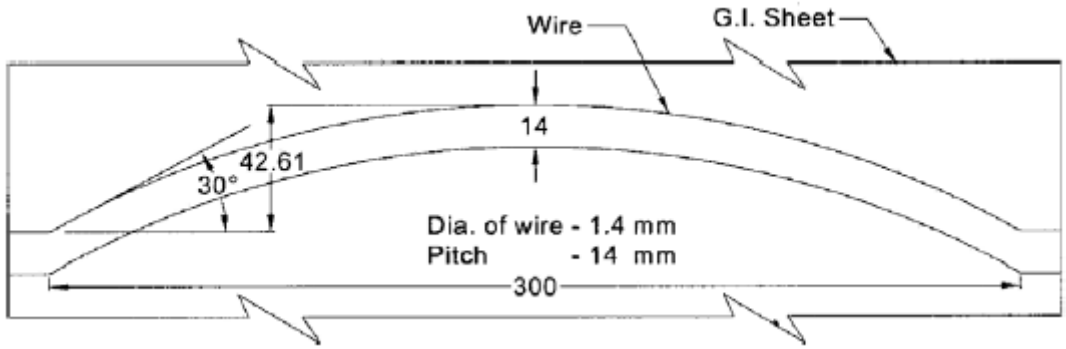

Figure 2.15 Orientation of Arc Shaped Rib[20]

It was found that Nusselt number increases up to 3.80 times corresponding to (α/90) = 0.3333 and e/D = 0.0422 but friction factor increases only up to 1.75 times under the same operating conditions.

12 Combination of Inclined and Transverse Ribs

Varun et.al (2008) performed experiment by using combination of inclined and transverse ribs as the roughness element. It was found that relative roughness pitch (p/e) of 8 gave the best thermal performance. The geometry used is shown below in figure 2.16.

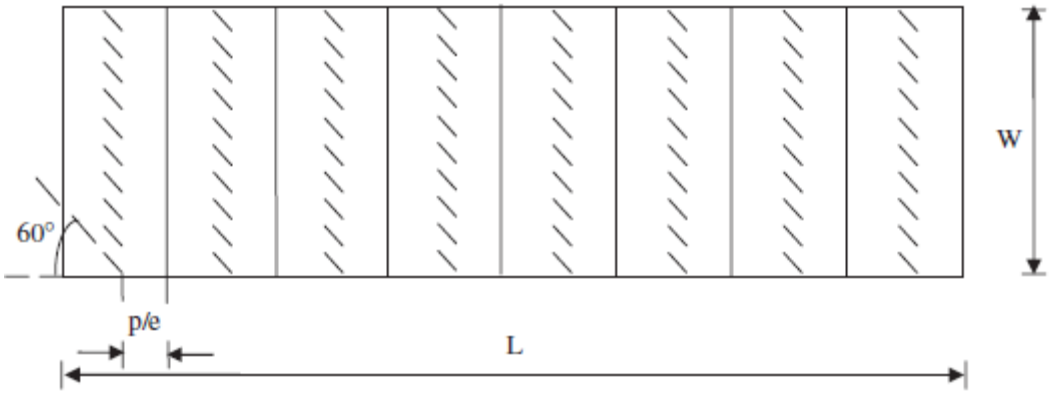

Figure 2.16 Orientation of Combination of Inclined and Transverse Ribs[24]

2.2.4 Thermal Efficiency of Solar Air Heater

Thermal efficiency of solar air heater is defined as the ratio of useful thermal gain to the incident solar radiation on the collector panel. Thermal efficiency of solar air heater is calculated without considering the effect of pumping power required for the flow of air into the solar air heater and it is given by the relation

$$\eta_{th} = \frac{q_u}{I\ A_C} \tag{2.1}$$

2.2.5 Effective Efficiency of Solar Air Heater[4]

The thermal performance of solar air heater is increased by having roughness on the absorber plate but in spite of increase in thermal performance there was considerable increase in pumping power requirement because more pump work was required to force the air into the duct. So selection of roughness geometry should be based on the parameter that taken in to account both the thermal and hydraulic performance.

Cortes & Piacentini [4] defined an effective efficiency of solar air heater on the basis of net thermal energy gain obtained from subtracting the thermal energy that will be required to overcome friction power from the collector useful gain. The formula for effective efficiency will be

$$\eta_{eff} = (q_u - P/C) / (IA_C) \tag{2.2}$$

Where C is the conversion efficiency (mechanical power, P to thermal) and its value is taken as 0.2. The rate of useful thermal gain (q_u) and mechanical power (P) consumed was obtained from relation:

$$q_u = F'[I(\tau\alpha) - U_L(t_o - t_i)/2]A_C \tag{2.3}$$

Where

$$F' = h / (h + U_L) \tag{2.4}$$

Where ‘h’ is calculated for different tupes of roughness geometries from the Nusselt number correlations as given in Table 2.1

and

$$P = VA\Delta P \quad (2.5)$$

Where$(\tau\alpha)$ is the transmittance absorptance product , $(t_o - t_i)$ is the fluid temperature rise & F' is the collector efficiency factor. The value of pressure drop across the collector having length (L) and velocity (V) & hydraulic diameter (D) is determined from relation:

$$\Delta P = 2fLV^2\rho / D \quad (2.6)$$

Where 'f' is the friction factor which is determined by using the correlations as given in Table 2.1

The correlations for Nusselt number and friction factor is given by table 2.1 shown below:

Table 2.1 Correlation for Nusselt number and friction factor[21]

Investigators	**Types of Roughness**	**Range of Operating Parameters**	**Correlations**
Momin et al.(2002)	V Shaped	p/e = 10 e/D = 0.02 to 0.034 α = 30°to 90° Re = 2500 to 18000	$f = 6.266*(Re)^{-0.425}(e/D)^{0.565}(\alpha/60°)^{-0.093}*Exp[-0.719*(ln\alpha/60°)^2]$ $Nu=0.067*(Re)^{0.888}(e/D)^{0.424}(\alpha/60°)^{0.077}*Exp[-0.782*(ln\alpha 60°)^2]$
Jaurker et al.(2006)	Grooved Rib	p/e = 4.5 to10 e/D=0.0181 to 0.0363 g/p = 0.3 to 0.7 Re= 3000 to 21000	$f=0.001227(Re)^{-0.199}(e/D)^{0.585}(p/e)^{7.19}(g/p)^{0.645}*[Exp\{-1.854(ln(p/e))^2\}]*[Exp\{1.513(ln(g/p))^2+0.8662(ln(g/p))^3\}]$ $Nu=0.002062(Re)^{0.936}(e/D)^{0.349}(P/e)^{3.318}*[Exp\{-0.868(ln(p/e))^2\}]*(g/p)^{1.108}*[Exp\{2.486(ln(g/p))^2+1.406(ln(g/p))^3\}]$

Contd…

Layek et al.(2007)	Chamfered Groove Rib	p/e 4.5 to 10 e/D= 0.022 to 0.04 g/p = 0.3 to 0.6 ϕ = 5° to 30° Re = 3000 to 21000	$f=0.00245(Re)^{-0.124}(e/D)^{0.365}(p/e)^{4.32}(g/p)^{-1.124}*[Exp(0.005)]*[Exp\{-^{1.09}(ln(p/e))^2\}]*[Exp\{-0.68(ln(g/p))^2\}]$ $Nu = 0.00225(Re)^{0.92}(e/D)^{0.52}(p/e)^{1.72}(g/p)^{-1.21}(\phi)^{1.24}*[Exp\{-0.22(ln\phi)^2\}]*[Exp\{-0.46(ln(p/e))^2\}]*[Exp\{-0.74(ln(g/p))^2\}]$
Karmare and Tikekar(2007)	Metal Grit Rib	p/e = 12.5 to 36 e/D = 0.035 to 0.044 l/s = 1to 1.72 Re = 4000 to 17000	$f = 15.55(Re)^{-0.26}(e/D)^{0.91}*(l/s)^{0.27}(p/e)^{-0.51}$ $Nu = 0.0024(Re)^{1.3}(e/D)^{0.42}(l/s)^{-0.146}(p/e)^{-0.27}$
Bopche and Tandale(2009)	Inverted U Shaped Turbulators	p/e = 6.667 to 57.14 e/D = 0.0186 to 0.03986 Re = 3800 to 18000	$f = 1.2134(Re)^{-0.2076}(p/e)^{-0.4259}(e/D)^{0.3285}$ $Nu = 0.5429(Re)^{0.7054}(p/e)^{-0.1592}(e/D)^{0.3619}$
Saini and Saini(2008)	Arc Shaped Wire	p/e = 10 e/D = 0.0213 to 0.0422 α /90 = 0.33 to 0.66 Re = 2000 to 17000	$f = 0.14408(Re)^{-0.17103}(e/D)^{0.1765}(\alpha/90)^{0.1185}$ $Nu = 0.00104(Re)^{1.3186}(e/D)^{0.3772}(\alpha/90)^{-0.1198}$

Contd…

Saini and Verma(2008)	Dimple Shaped Roughness	p/e = 8 to 12 e/D = 0.0189 to 0.038 Re = 2000 to 12000	$f=0.642(Re)^{-0.423}(p/e)^{-0.465}[Exp0.054 (\log(p/e))^2] * (e/D)^{-0.0124} [Exp0.840(\log(e/D))^2]$ $Nu = 0.00052(Re)^{1.27}(p/e)^{3.15}(e/D)^{0.033}*[Exp(-2.12)(\log(p/e))^2]*[Exp(-1.30)(\log(e/D))^2]$
Varun et al.(2008)	Combination of Inclined and Transverse Ribs	p/e = 3 to 8 e/D = 0.030 Re = 2000 to 14000	$f = 1.0858(Re)^{-0.3685}(p/e)^{0.0114}$ $Nu = 0.0006(Re)^{1.213}(p/e)^{0.0104}$

CHAPTER 3

METHODOLOGY

3.1 METHODOLOGY

Methodology is divided into two parts:

- Mathematical Modelling
- Simulation

3.1.1 Mathematical Modelling

Here in this chapter first of all mathematical modelling is done to theoretically predict the performance of the solar collector provided with different artificial roughnesses. The solar collector subsystem is modeled by using heat energy balance equation which governs the solar collector performance. To develop the mathematical model following assumptions were made.

- Constant solar irradiation of 1000W/m^2.
- Collector area is constant.
- The base plate temperature is constant.
- Absorber plate material is black painted aluminium.
- Ambient air temperature of 27°C.
- The sides and bottom of the solar collector is perfectly insulated.

In order to determine the effective efficiency of solar collector provided with artificial roughness on its absorber plate following equations are used.

Thermal Efficiency of Solar Air Heater

Thermal efficiency of solar air heater is defined as the ratio of useful thermal gain to the incident solar radiation on the collector panel. Thermal efficiency of solar air heater is calculated without considering the effect of pumping power required for the flow of air into the solar air heater and it is given by the relation

$$\eta_{th} = \frac{q_u}{I\ A_C} \tag{3.1}$$

When the mathematical model developed, analyze the performance (in terms of effective efficiency) of solar collector provided with different roughness geometries and after that select the optimum design.

Effective Efficiency of Solar Air Heater[4]

The thermal performance of solar air heater is increased by having roughness on the absorber plate but in spite of increase in thermal performance there was considerable increase in pumping power requirement because more pump work was required to force the air into the duct. So selection of roughness geometry should be based on the parameter that taken in to account both the thermal and hydraulic performance.

Cortes & Piacentini[4] defined an effective efficiency of solar air heater on the basis of net thermal energy gain obtained from subtracting the thermal energy that will be required to overcome friction power from the collector useful gain. The formula for effective efficiency will be:

$$\eta_{eff} = (q_u - P/C)/(IA_C) \quad (3.2)$$

Where c is conversion efficiency (mechanical power, P to thermal) and its value is taken as 0.2. The rate of useful thermal gain (q_u) and mechanical power (P) consumed was obtained from relation:

$$q_u = F'[I(\tau\alpha) - U_L(t_o - t_i)/2]A_C \quad (3.3)$$

Where

$$F' = h / (h + U_L) \quad (3.4)$$

Where h is calculated for different roughness geometries form the Nusselt number correlations as given in Table 2.1

and

$$P = VA\Delta P \quad (3.5)$$

Where$(\tau\alpha)$ is the transmittance absorbtance product & $(t_o - t_i)$ is the fluid temperature rise & F' is the collector efficiency factor. The value of pressure drop across the collector having length (L) and velocity (V) & hydraulic diameter (D) is determined from relation.

$$\Delta P = 2fLV^2\rho / D \quad (3.6)$$

Table 3.1 Typical Values of System and Operating Parameters[21]

Parameters	values
Length L (mm)	1000
Height H (mm)	20
Width W (mm)	200
Insolation I (W/m^2)	1000
Transmittance-absorbtance ($\tau\alpha$)	0.85
Overall loss coefficient $U_L(W/m^{2\circ}C)$	5

3.2 Simulation

FEM simulation software, ANSYS version 12(workbench mode) has been used for simulation. Fluid flow (FLUENT) module has been used in present work. Fluid flow (FLUENT) module predicts the outlet temperature, velocity, flow behavior to great accuracy due to application of thermal loading on the work piece. Different types of thermal loading that can be applied on the work piece in Fluid flow (FLUENT) module are temperature, convection, radiation and heat flux.

Various steps involved in the simulation procedure are as follows

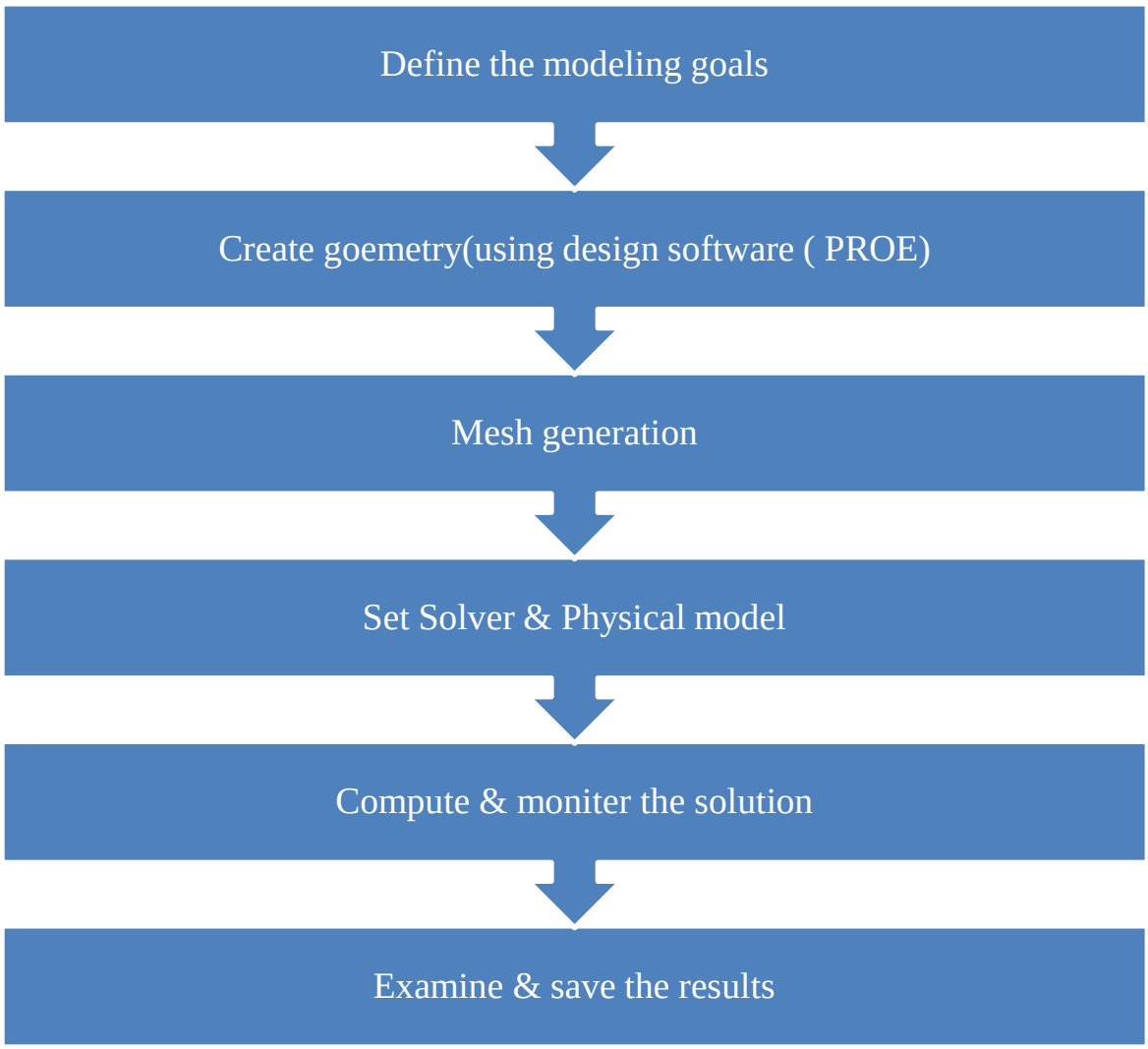

Figure 3.1. Steps Involved in the FLUENT Analysis Procedure[10]

3.2.1 Simulation of a Roughened Solar Air Heater

Using the Fluid flow (FLUENT) module of ANSYS heat transfer analysis was conducted on the solar air heater provided with different types of artificial roughness on its absorber plate. The main aim of this analysis is to solve the heat transfer that take place from absorber plate to moving air in the solar air heater. This simulation module predicts the velocity and outlet temperature of the air. Finally the result obtained from simulation is compared with the result obtained from mathematical modeling

3.2.1.1 Assumptions for Modeling

For this analysis few assumptions are made which are as follows:

1. Inlet air and ambient air temperature is 27°C.
2. Constant heat flux of 1000W/m^2 is applied uniformly on absorber plate.
3. The air is assumed to be an ideal gas.
4. The system is perfectly insulated and there is no heat loss to the surroundings.
5. The flow of air is steady, turbulent &three dimensional.
6. The thermal conductivity of duct wall &roughness material does not vary with temperature.

3.2.1.2 Details of the Solar Air Heater

The cross sectional dimension of the duct considered for this analysis are 200mm x 20mm respectively as shown in figure 3.2. The aspect ratio has been kept 10 for this analysis. The flow system consists of 1000mm long test section and a constant heat flux of 1000W/m^2 is applied on the absorber plate. The geometry of solar air heater is same for all the roughnesses under investigation.

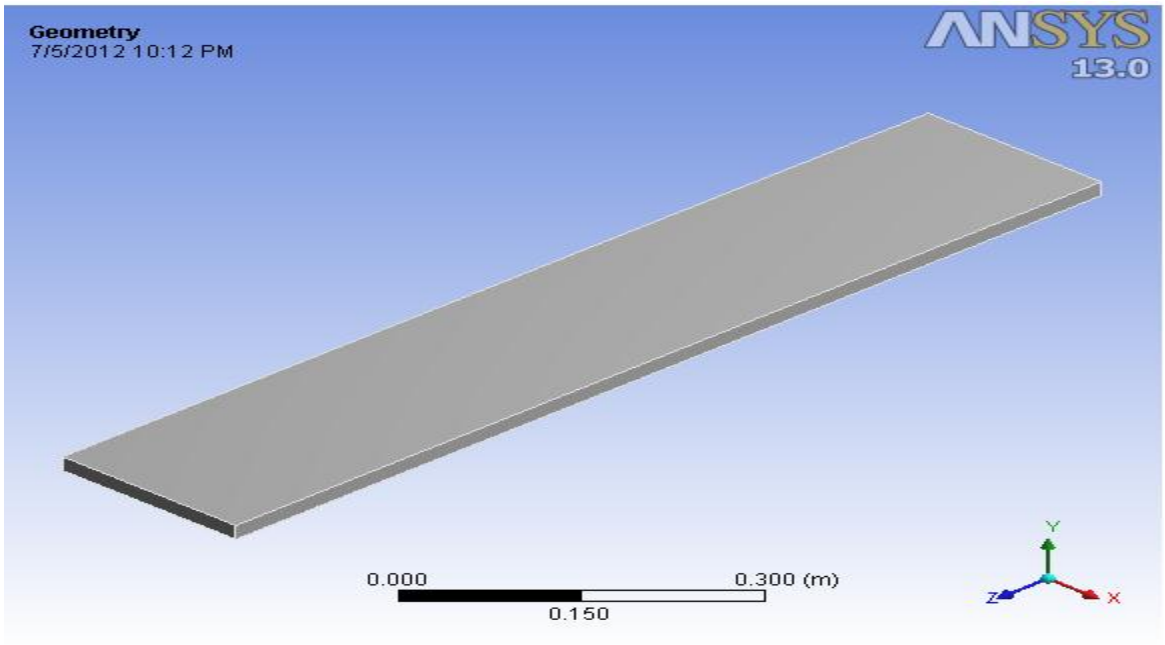

Figure 3.2 Solar Air Heater Geometry

3.2.2 Simulation of Solar Air Heater Provided with V Shaped Ribs

3.2.2.1 Geometric Modeling

Solar air heater duct modeled with dimensions of 1000 x 200 x 20 mm respectively. Thickness of absorber plate is 0.5 mm. Roughness is considered on the underside of the absorber plate while the remaining three sides is considered as a smooth surface as shown in figure 3.3.

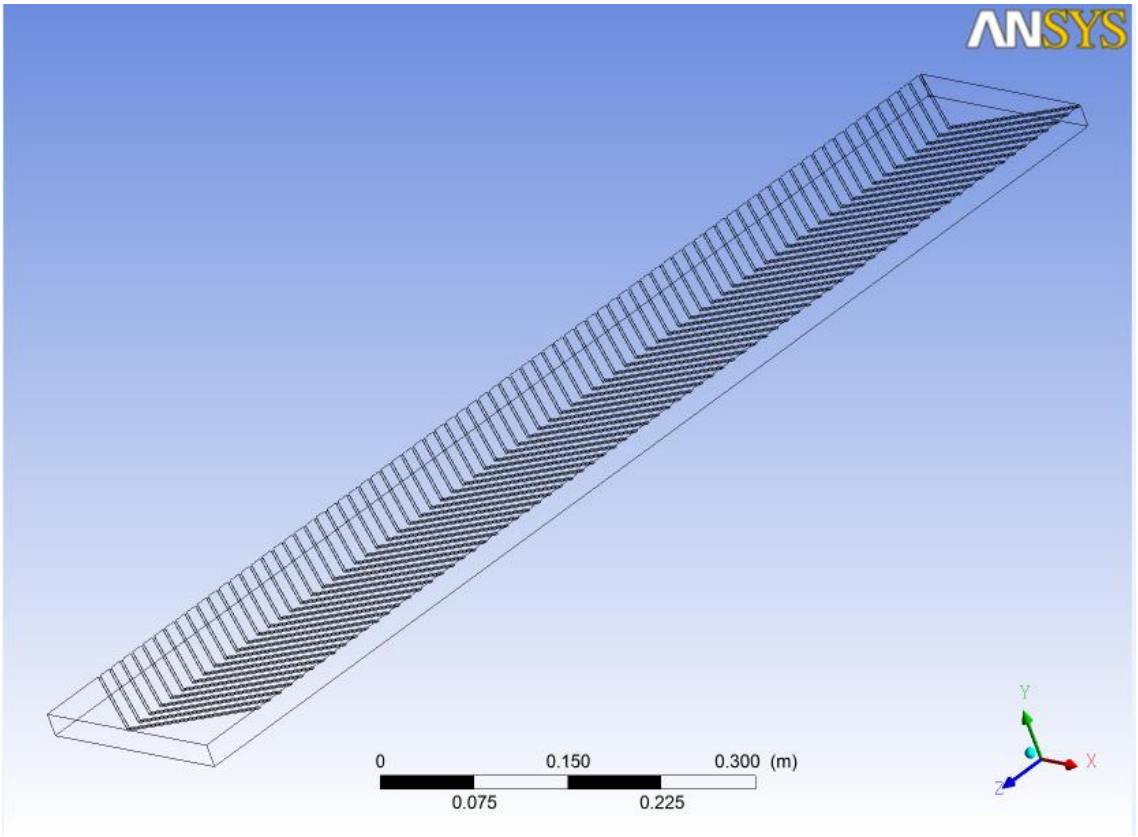

Figure 3.3 Geometric Model (V Shaped Ribs)

Copper wire in the form of V shaped ribs is considered as a roughness element on the underside of the absorber plate. The material for absorber plate is aluminium and angle of attack (α) is 60°.The values of relative roughness height (e/D) and relative roughness pitch (P/e) considered for this analysis are 0.035 and 10 respectively. The range of Reynolds's number is ranging from 2500-18000.

3.2.2.2 Meshing

Tetrahedral (Patch independent) mesh method is used as shown in figure 3.4. Table 3.2 gives the mesh detail.

Table 3.2 Mesh Characteristics (V Shaped Ribs)

Type of element	Tetrahedral
Number of nodes	158003
Number of elements	793667

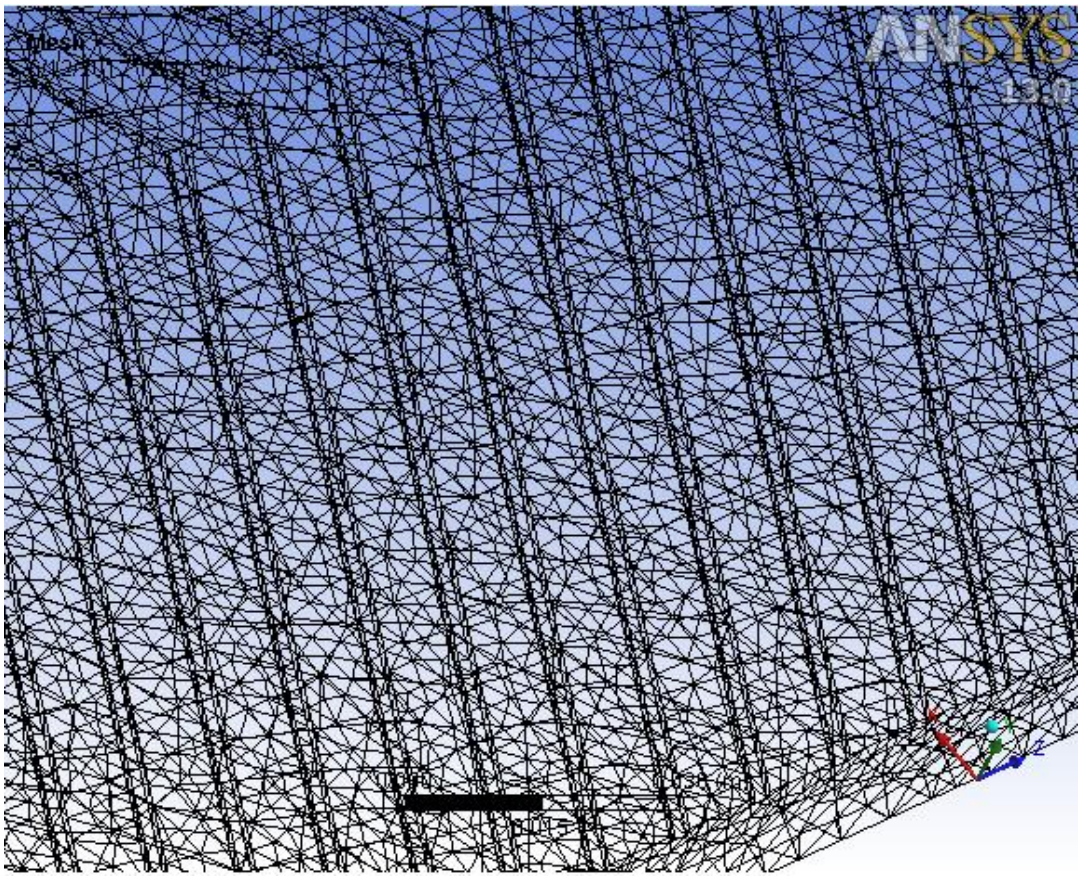

Figure 3.4 Mesh Details (V Shaped Ribs)

3.2.2.3 Boundary Conditions

To analyze the flow and heat transfer 3-D model has been set up instead of 2-D model for the selected geometry because secondary flow takes place. k - ε with turbulence intensity (5%) is used in place of Shear Stress Transport(SST) model to model turbulence because SST model is more complex and the result obtained from both models is quite similar. To control the radiation intensity & direction a discrete ordination (DO) irradiation model is used & also employs the energy equation. The various boundary conditions employed are given in table 3.3.

Table 3.3 Boundary Conditions (V Shaped Ribs)

Location	**Boundary Type**	**Boundary Details**
• Air inlet	Velocity Inlet	Velocity – 1.76 m/sec Temperature – 300K
• Outlet	Outflow	Temperature – 315.69K
• Insulation	Wall	No slip wall Adiabatic with no heat loss Material used - Wood.
• V shaped ribs	Wall	Heat Flux – 1000W/m^2 Material used – Copper • Emissivity -1.0 • Density-8978kg/m^3 • Thermal Conductivity – 387.6W/m/$^\circ$ C • Specific Heat – 381J/kg/$^\circ$ C

3.2.3 Simulation of Solar Air Heater Provided with Grooved Ribs

3.2.3.1 Geometric Modeling

The geometry of solar air heater duct is same as discussed above and thickness of absorber plate is also same that is 0.5mm. Roughness in the form of grooved ribs is created on the underside of absorber plate while the remaining three sides are considered as smooth surfaces as shown in figure 3.6. The material for absorber plate is aluminium and the values of relative roughness height (e/D), relative roughness pitch (p/e), relative groove position (g/p) considered for this analysis are 0.034, 10 and 0.7 respectively. The value of Reynolds's number ranges from 3000-21000.

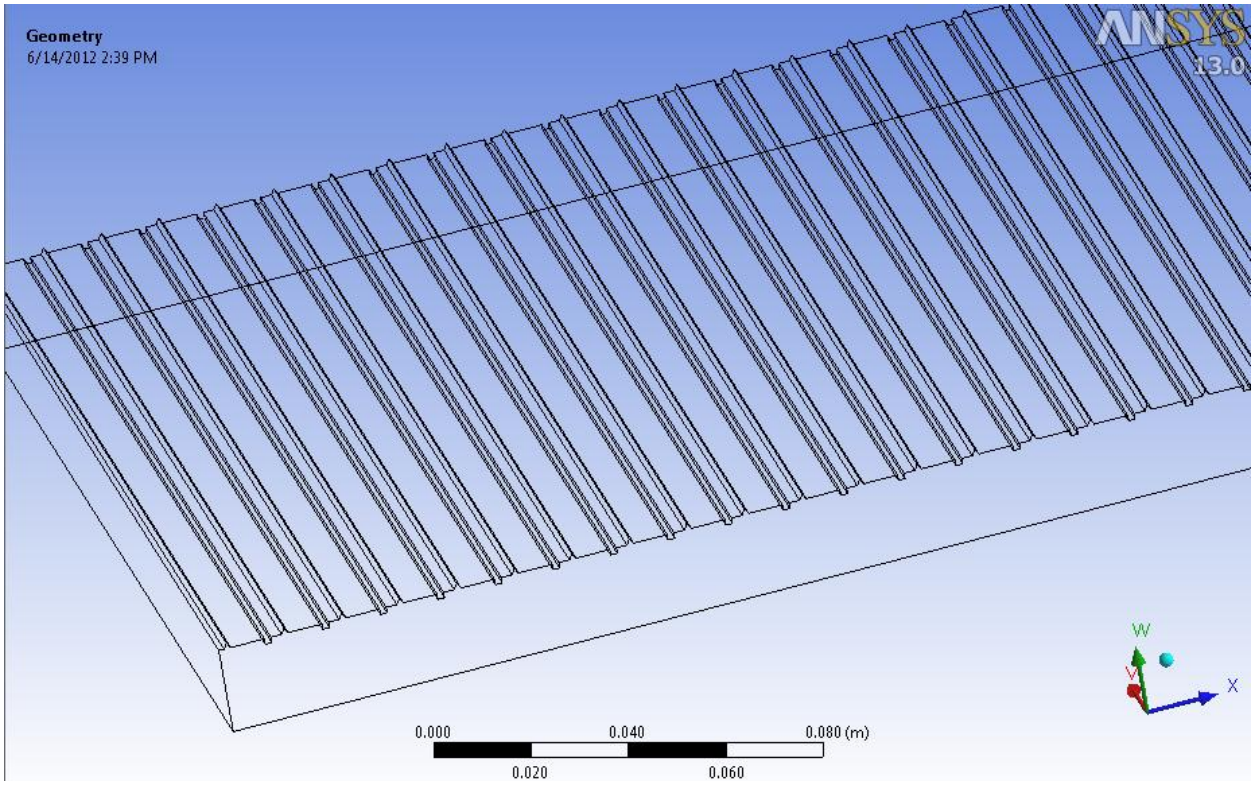

Figure 3.5 Geometric Model (Grooved Ribs)

3.2.3.2 Meshing

Tetrahedral (Patch independent) mesh method is used as shown in figure 3.7. Table 3.4 gives the mesh detail.

Table 3.4 Mesh Characteristics (Grooved Ribs)

Type of element	Tetrahedral
Number of nodes	183039
Number of elements	922176

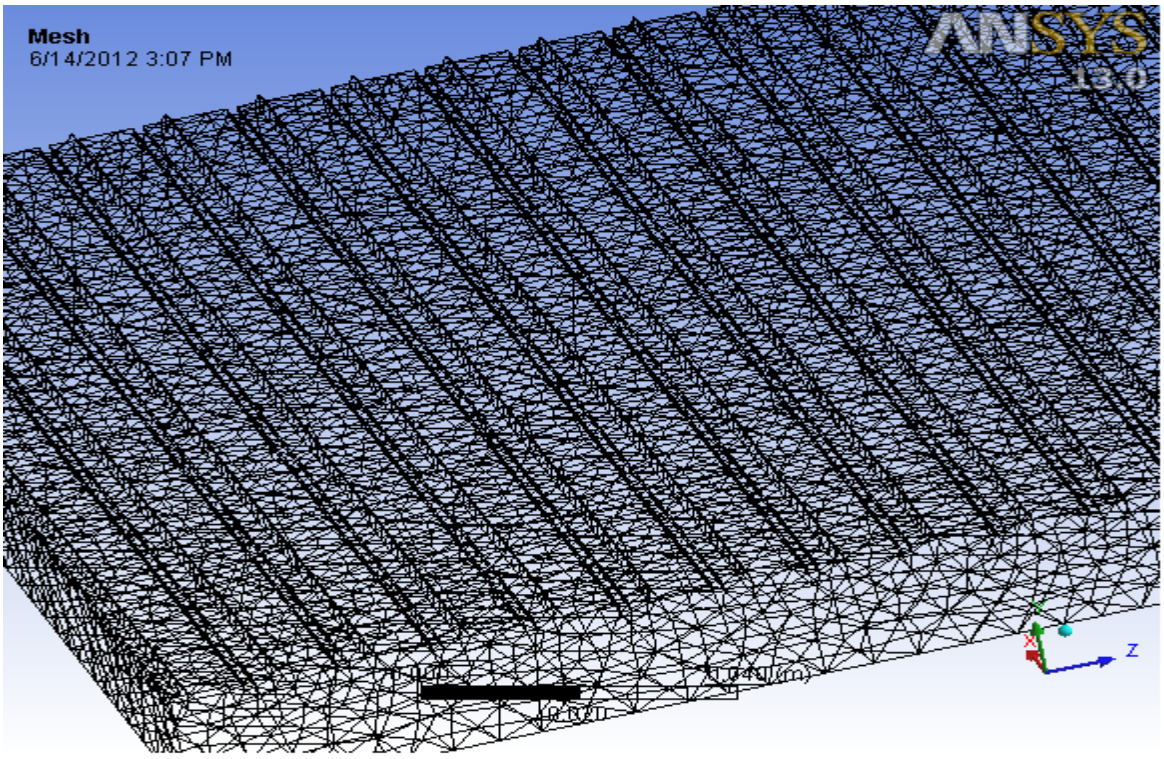

Figure 3.6 Mesh Details (Grooved Ribs)

3.2.3.3 Boundary Conditions

The various boundary conditions employed are given below in table 3.5

Location	Boundary Type	Boundary Details
• Air Inlet	Velocity Inlet	Velocity – 5.72 m/sec Temperature – 300K
• Outlet	Outflow	Temperature – 338K
• Insulation	Wall	No slip wall Adiabatic with no heat loss Material used - Wood.
• Grooved Ribs	Wall	Heat Flux – 1000W/m^2 Material used – Aluminium • Emissivity -1.0 • Density-2719kg/m^3 • Thermal Conductivity – 202.4W/m/$^\circ$ C • Specific Heat – 871J/kg/$^\circ$ C

3.2.4 Simulation of Solar Air Heater Provided with Chamfered Grooved Ribs

3.2.4.1 Geometric Modeling

The geometry of solar air heater duct is same as discussed above and thickness of absorber plate is also same that is 0.5mm. Roughness in the form of chamfered ribs grooved on the underside of absorber plate is created while the remaining three sides are considered as smooth surfaces as shown in figure 3.9. The material for absorber plate is aluminium and the values of relative roughness height (e/D), relative roughness pitch (p/e), relative groove position (g/p), chamfer angle (ϕ) considered for this analysis are 0.034, 10, 0.6 and 30° respectively. The value of Reynolds's number ranges from 3000-21000.

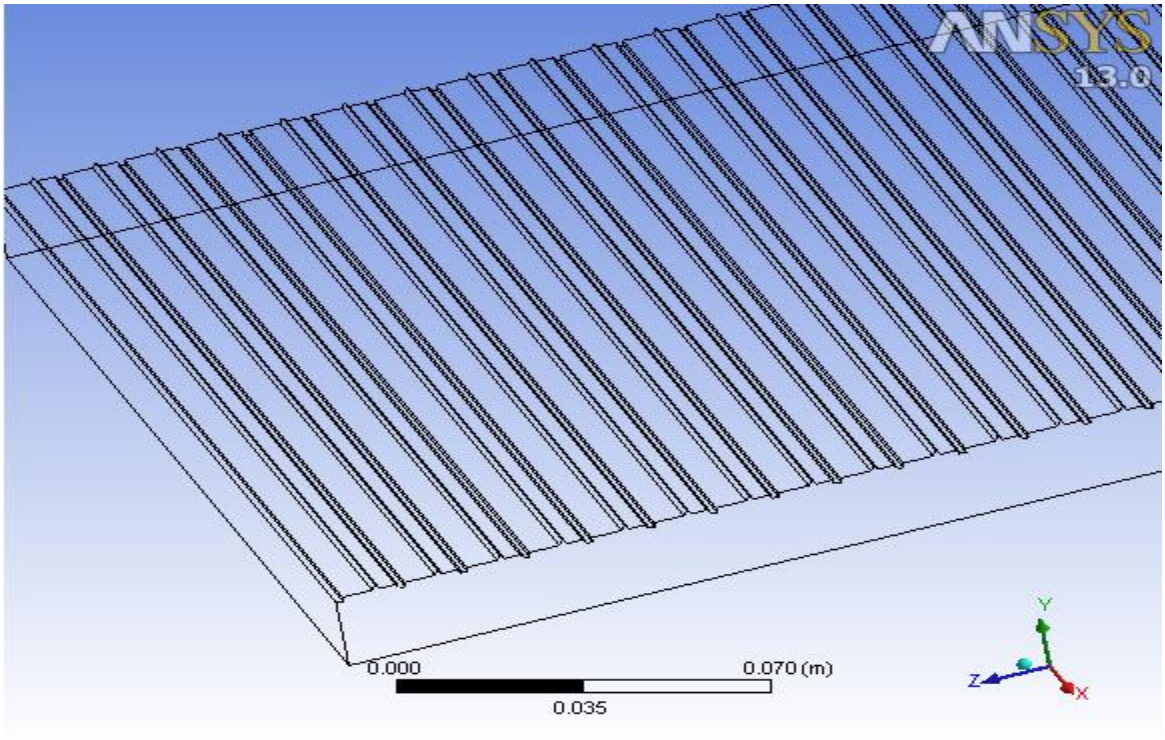

Figure 3.7. Geometric Model (Chamfered Ribs Grooved)

3.2.4.2 Meshing

Tetrahedral (Patch independent) mesh method is used as shown in figure 3.10. Table 3.6 gives the mesh detail

Table3.6 Mesh Characteristics (Chamfered Ribs Grooved)

Type of element	Tetrahedral
Number of nodes	187342
Number of elements	950006

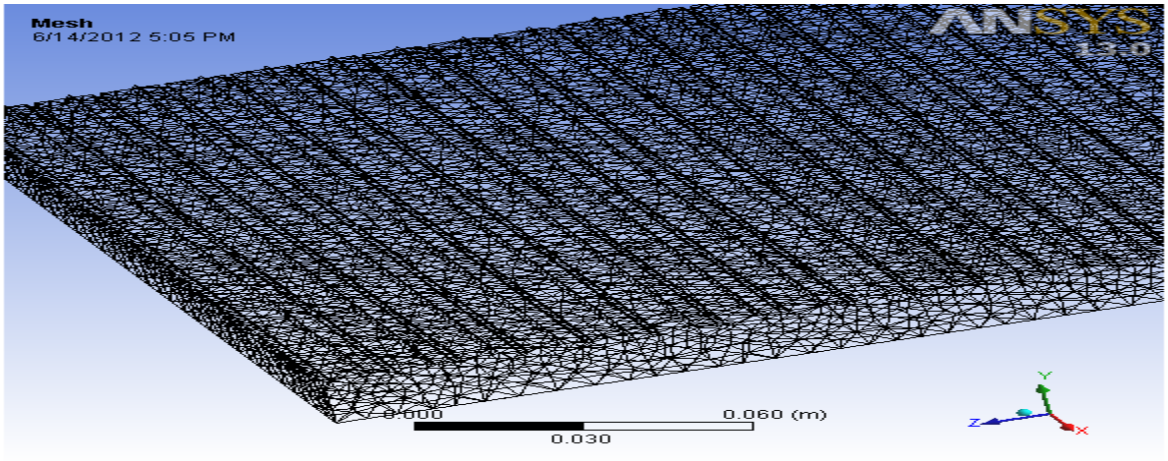

Figure 3.8 Mesh Details (Chamfered Ribs Grooved)

3.2.4.3 Boundary Conditions

The various boundary conditions employed are given below in table 3.7

Location	**Boundary Type**	**Boundary Details**
• Air Inlet	Velocity Inlet	Velocity – 5.72 m/sec Temperature – 300K
• Outlet	Outflow	Temperature – 305.79K
• Insulation	Wall	No slip wall Adiabatic with no heat loss Material used - Wood.
• Chamfered Grooved Ribs	Wall	Heat Flux – 1000W/m^2 Material used – Aluminium • Emissivity -1.0 • Density-2719kg/m^3 • Thermal Conductivity – 202.4W/m/$^\circ$ C • Specific Heat – 871J/kg/$^\circ$ C

3.2.5 Simulation of Solar Air Heater Provided with Dimple Shaped Ribs

3.2.5.1 Geometric Modeling

The geometry of solar air heater duct is same as discussed above and thickness of absorber plate is also same that is 0.5mm. Roughness in the form of dimple shaped ribs on the underside of absorber plate is created while the remaining three sides are considered as smooth surfaces as shown in figure 3.12. The material for absorber plate is aluminium and the values of relative roughness height (e/D) and relative roughness pitch (p/e) considered for this analysis are 0.034 and 12 respectively. The value of Reynolds's number ranges from 2000-12000.

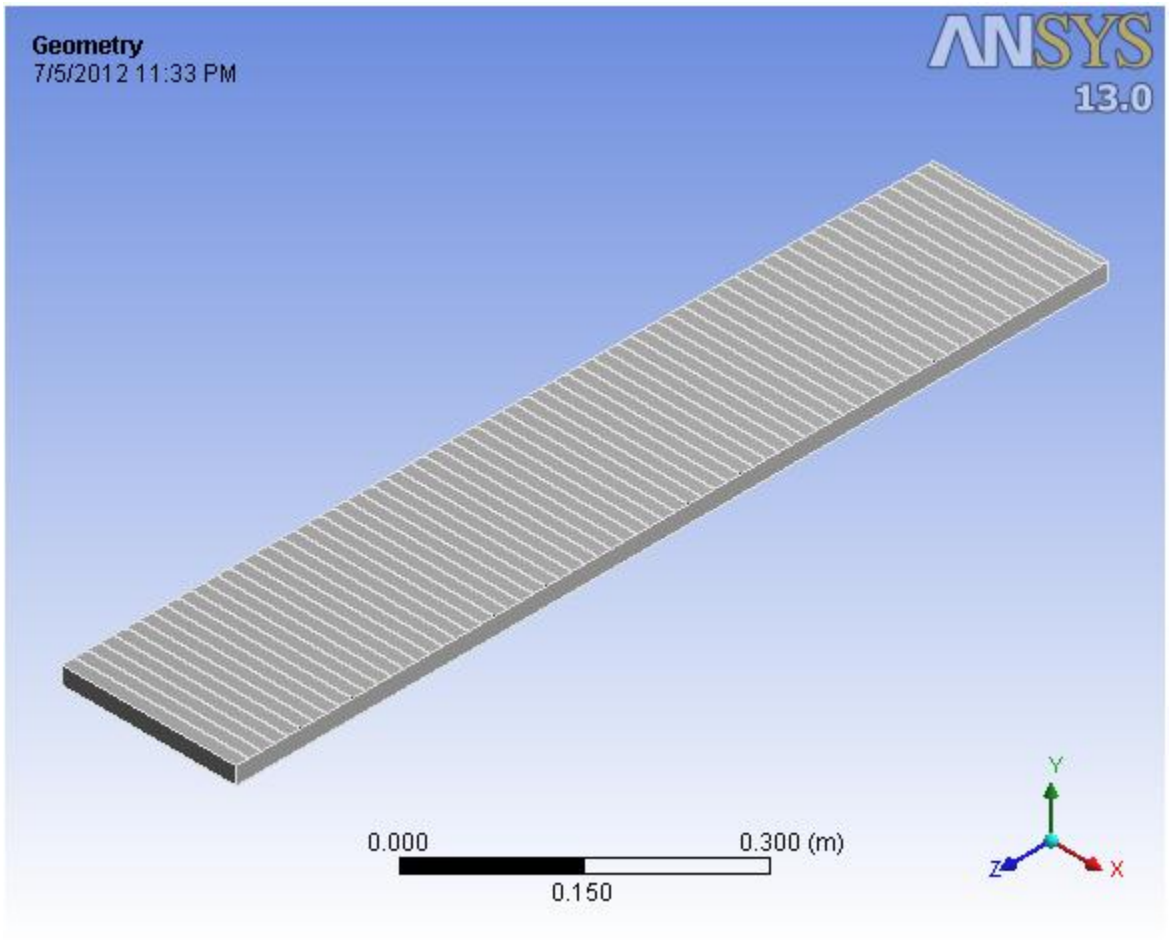

Figure 3.9 Geometric Model (Dimple Shaped Ribs)

3.2.5.2 Meshing

Tetrahedral (Patch independent) mesh method is used as shown in figure 3.13. Table 3.8 gives the mesh detail

Table 3.8 Mesh Characteristics (Dimple Shaped Ribs)

Type of element	Tetrahedral
Number of nodes	74295
Number of elements	374679

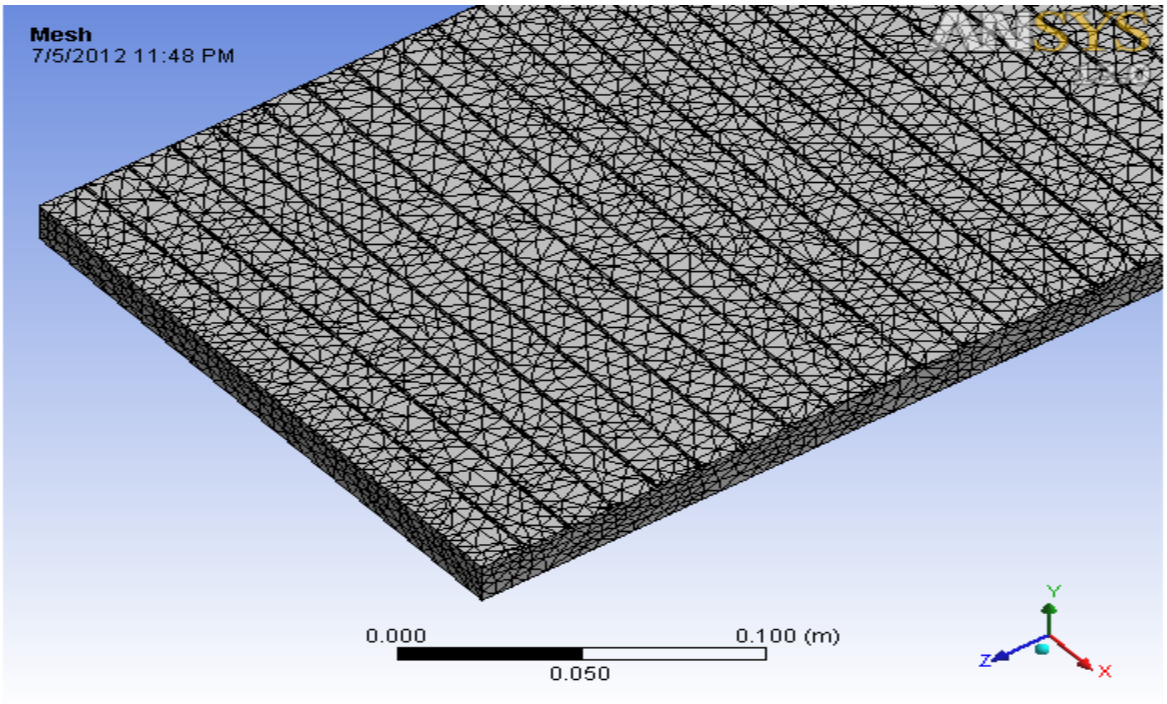

Figure 3.10 Mesh Details (Dimple Shaped Ribs)

3.2.5.3 Boundary Conditions

The various boundary conditions employed are given below in table 3.9

Table3.9 Boundary conditions (Dimple Shaped Ribs)

Location	**Boundary Type**	**Boundary Details**
• Air Inlet	Velocity Inlet	Velocity – 5.28 m/sec Temperature – 300K
• Outlet	Outflow	Temperature – 318.87K
• Insulation	Wall	No slip wall Adiabatic with no heat loss Material used - Wood.
• Dimple Shaped Ribs	Wall	Heat Flux – 1000W/m^2 Material used – Aluminium • Emissivity -1.0 • Density-2719kg/m^3 • Thermal Conductivity – 202.4W/m/$^\circ$ C • Specific Heat – 871J/kg/$^\circ$ C

3.2.6 Simulation of Solar Air Heater Provided with U Shaped Turbulators

3.2.6.1 Geometric Modeling

The geometry of solar air heater duct is same as discussed above and thickness of absorber plate is also same that is 0.5mm. Roughness in the form of U shaped turbulators on the underside of absorber plate is created while the remaining three sides are considered as smooth surfaces as shown in figure 3.15. The material for absorber plate is aluminium and the values of relative roughness height (e/D) and relative roughness pitch (p/e) considered for this analysis are 0.034 and 57.14 respectively. The value of Reynolds's number ranges from 3800-18000.

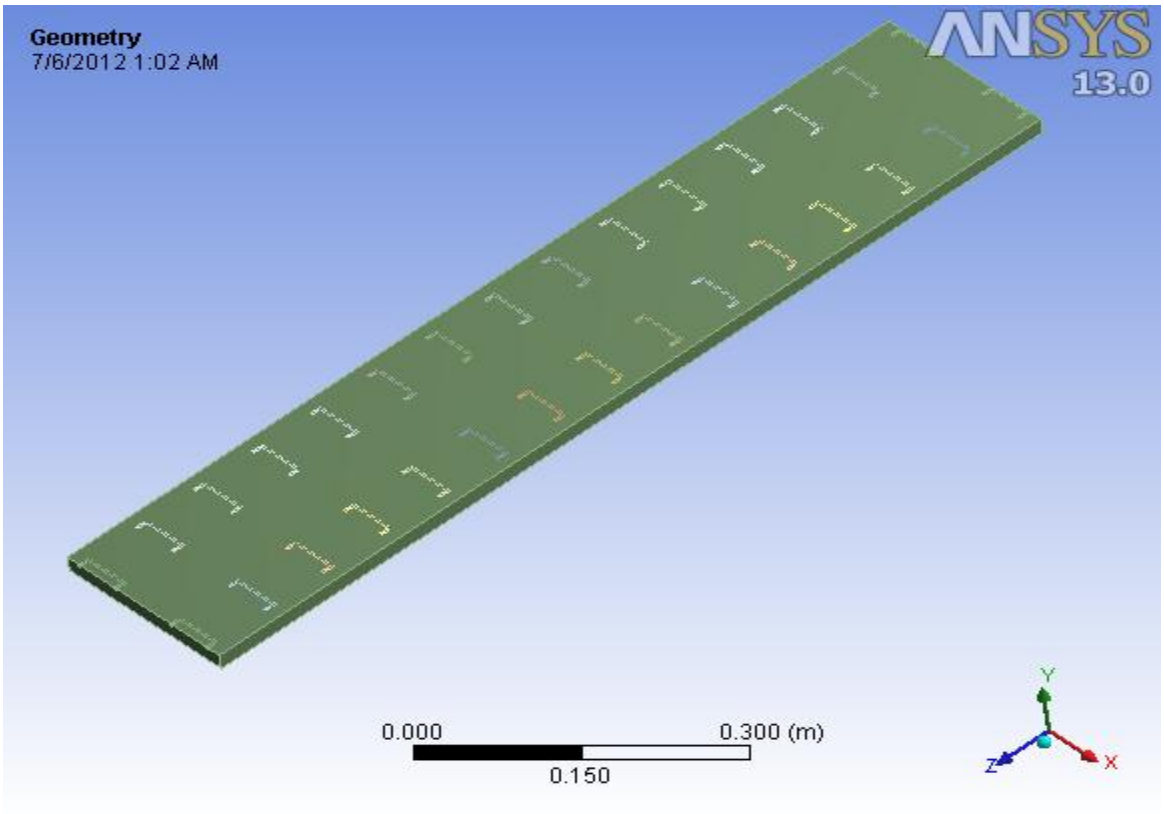

Figure 3.11 Geometric Model (U Shaped Turbulators)

3.2.6.2 Meshing

Tetrahedral (Patch independent) mesh method is used as shown in figure 3.16. Table 3.10 gives the mesh detail

Table 3.10 Mesh Characteristics (U Shaped Turbulators)

Type of element	Tetrahedral
Number of nodes	117903
Number of elements	530712

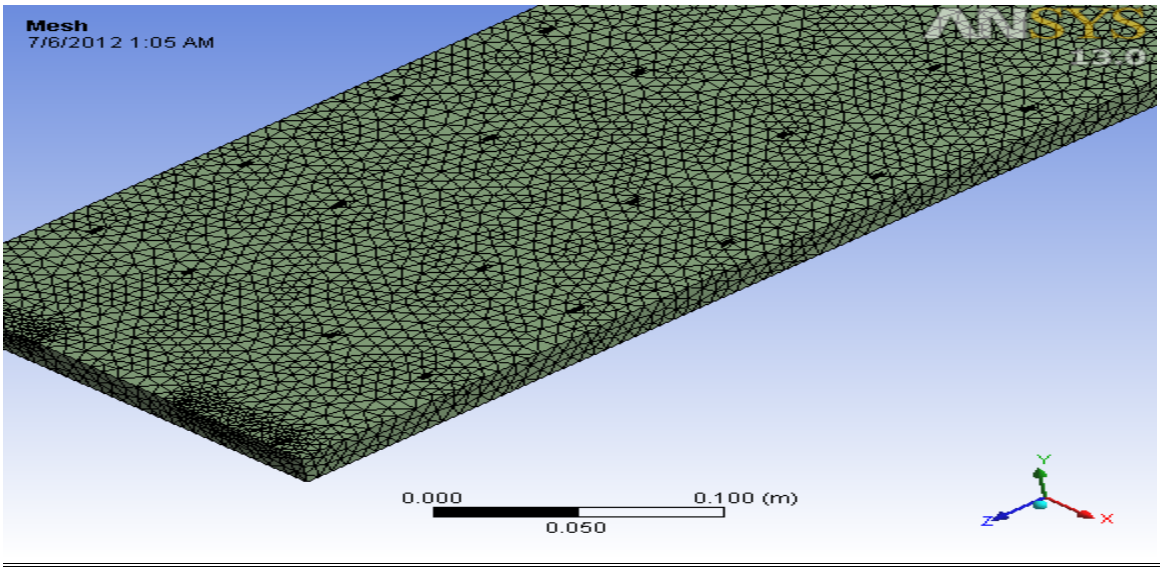

Figure 3.12 Mesh Details (U Shaped Turbulators)

3.2.6.3 Boundary Conditions

The various boundary conditions employed are given below in table 3.11

Table 3.11 Boundary conditions (U Shaped Turbulators)

Location	Boundary Type	Boundary Details
• Air Inlet	Velocity Inlet	Velocity – 7.04 m/sec Temperature – 300K
• Outlet	Outflow	Temperature – 315.91K
• Insulation	Wall	No slip wall Adiabatic with no heat loss Material used - Wood.
• Dimple Shaped Ribs	Wall	Heat Flux – 1000W/m^2 Material used – Aluminium • Emissivity -1.0 • Density-2719kg/m^3 • Thermal Conductivity – 202.4W/m/$^\circ$ C • Specific Heat – 871J/kg/$^\circ$ C

CHAPTER 4

RESULTS AND DISCUSSIONS

4.1 MATHEMATICAL MODELLING RESULTS

In present work following the mathematical modelling methodology and utilizing the governing equations as discussed in detail in Chapter 3, following sets of results were obtained.

1. Effective efficiency of solar air heater provided with different types of roughness on its absorber plate.
2. Effective efficiency of artificially roughened solar air heater at different relative roughness element height for the optimal values of other parameters.
3. Comparison of effective efficiency for solar air heater provided with different types of roughness on its absorber plate at particular value of relative roughness height i.e. 0.034.

4.1.1 Effective Efficiency of Solar Air Heater Provided with V Shaped Ribs

Figure 4.1 shows the variation of effective efficiency w.r.t Reynolds's number for solar air heater provided with V shaped ribs as a roughness element on its absorber plate.

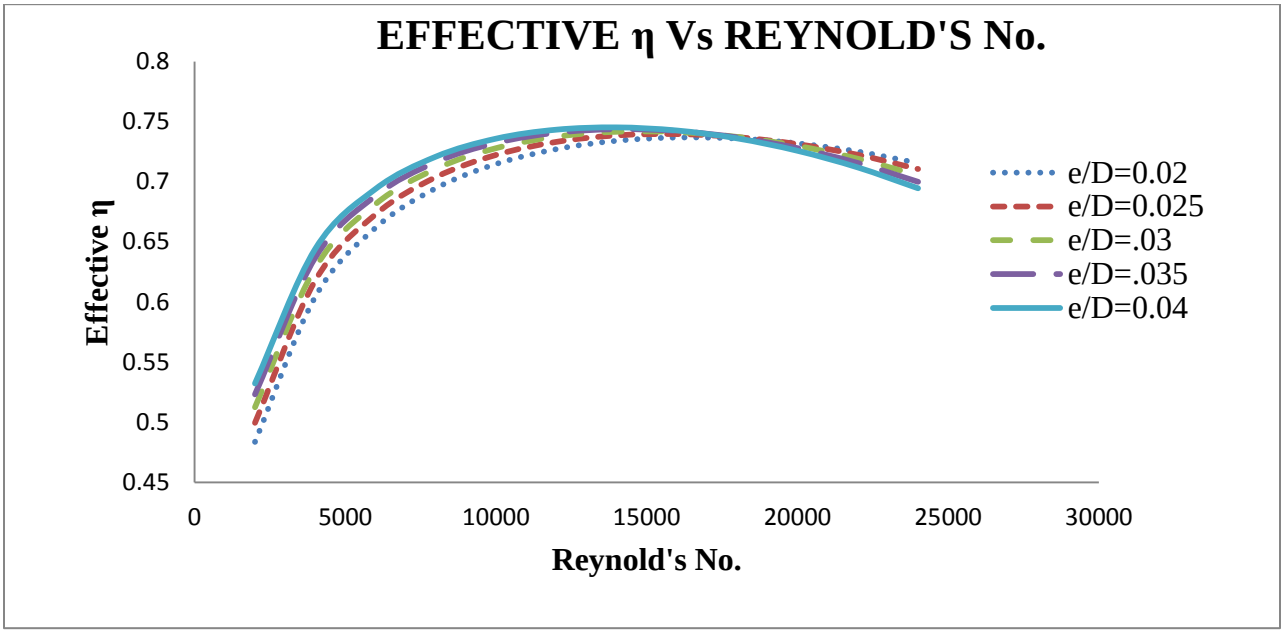

Figure 4.1 Variation of Effective Efficiency with Reynolds's No.(V Shaped Ribs)

From the figure 4.1 it is clear that initially effective efficiency increases with Reynolds's number for all relative roughness height (e/D) and attains corresponding maximum values and after that it starts decreasing this is may be due to the dominance of mechanical power. In this case value of relative roughness pitch (p/e) is 10 for all the relative roughness height (e/D). It was also observed that at lower Reynolds's no. higher values of relative roughness height gives better effective efficiency and at higher Reynolds's no. lower value of relative roughness height give better efficiency. It was also found that effective efficiency attains a maximum value of approx. 0.074 at Reynolds's no. of 14000 for relative roughness height of 0.04.

4.1.2 Effective Efficiency of Solar Air Heater Provided with Grooved Ribs

Figure 4.2 shows the variation of effective efficiency w.r.t Reynolds's number for solar air heater provided with grooved ribs as a roughness element on its absorber plate.

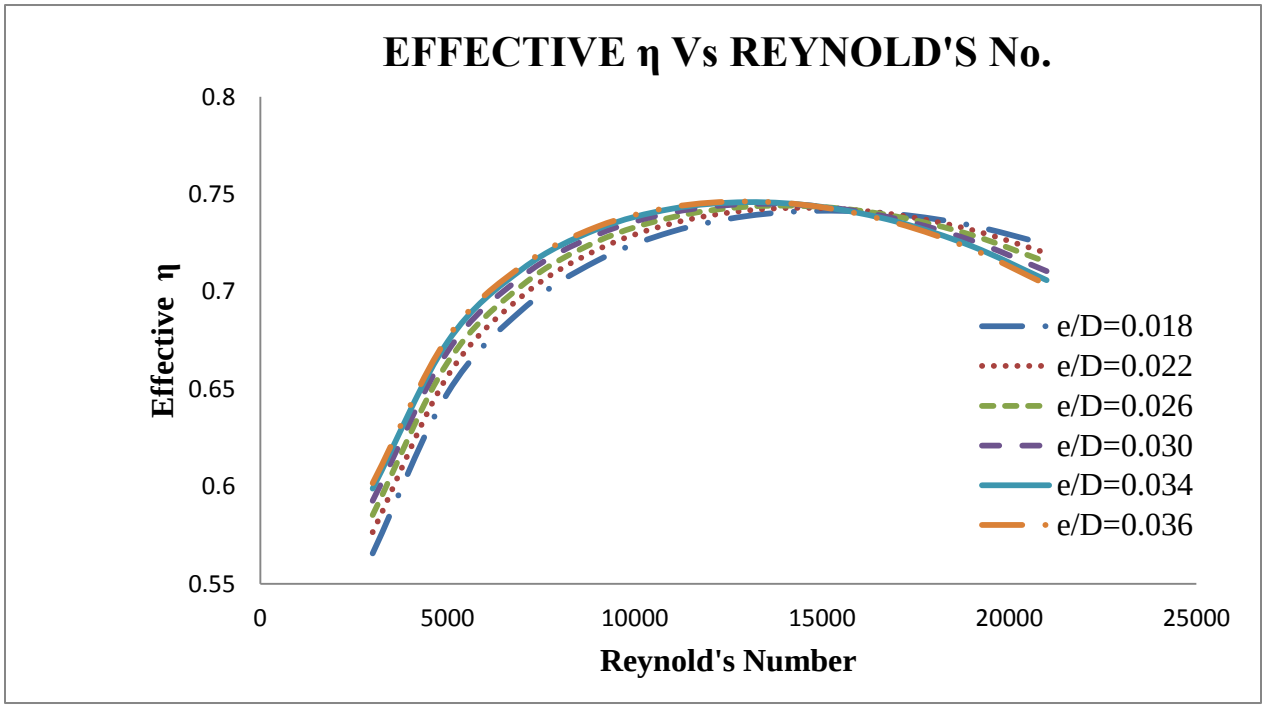

Figure 4.2 Variation of Effective Efficiency with Reynolds's No. (Grooved Ribs)

From the figure 4.2 it is clear that initially effective efficiency increases with Reynolds's number for all relative roughness height (e/D) and attains corresponding maximum values and after that it starts decreasing slightly. In this case value of relative roughness pitch (p/e) is 10 and value of

relative groove position (g/p) is 0.7 for all the relative roughness height (e/D). It was also observed that at lower Reynolds's no. higher values of relative roughness height gives better effective efficiency and at higher Reynolds's no. lower value of relative roughness height give better efficiency. It was also found that effective efficiency attains a maximum value of approx. 0.7463 at Reynolds's no. of 13000 for relative roughness height of 0.036.

4.1.3 Effective Efficiency of Solar Air Heater Provided with Chamfered Grooved Ribs

Figure 4.3 shows the variation of effective efficiency w.r.t Reynolds's number for solar air heater provided with chamfered grooved ribs as a roughness element on its absorber plate.

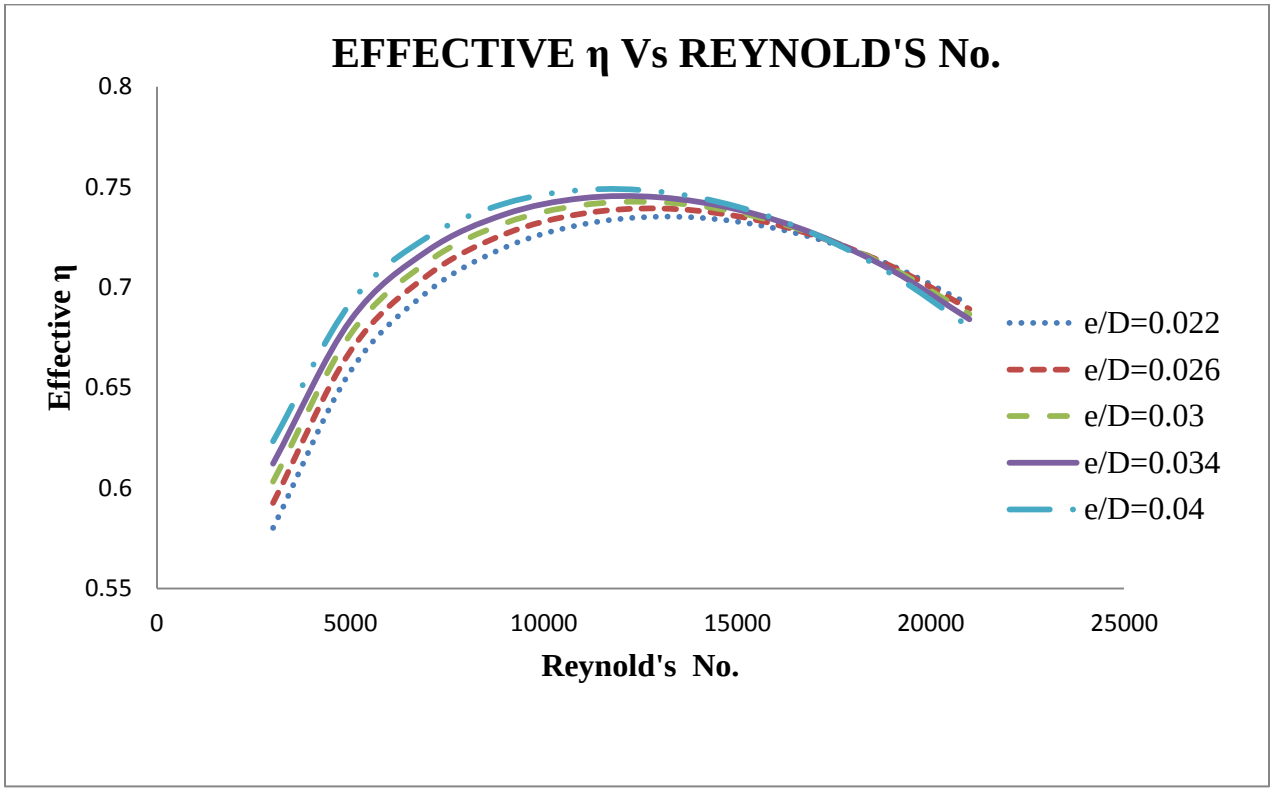

Figure 4.3 Variation of Effective Efficiency with Reynolds's No. (Chamfered Grooved Ribs)

From the figure 4.3 it is clear that initially effective efficiency increases with Reynolds's number for all relative roughness height (e/D) but the rate at of increase of effective efficiency decrease with increase of Reynolds's number and after that it starts decreasing slightly. In this case value of relative roughness pitch (p/e) is 10 and value of relative groove position (g/p) and chamfer angle (ϕ) is 0.6 and 30° respectively for all the relative roughness height (e/D). It was also

observed that at lower Reynolds's no. higher values of relative roughness height gives better effective efficiency and at higher Reynolds's no. lower value of relative roughness height give better efficiency. It was also found that effective efficiency attains a maximum value of approx. 0.7485 at Reynolds's no. of 11000 for relative roughness height of 0.04.

4.1.4 Effective Efficiency of Solar Air Heater Provided with Dimple Shaped Ribs

Figure 4.4 shows the variation of effective efficiency w.r.t Reynolds's number for solar air heater provided with chamfered grooved ribs as a roughness element on its absorber plate.

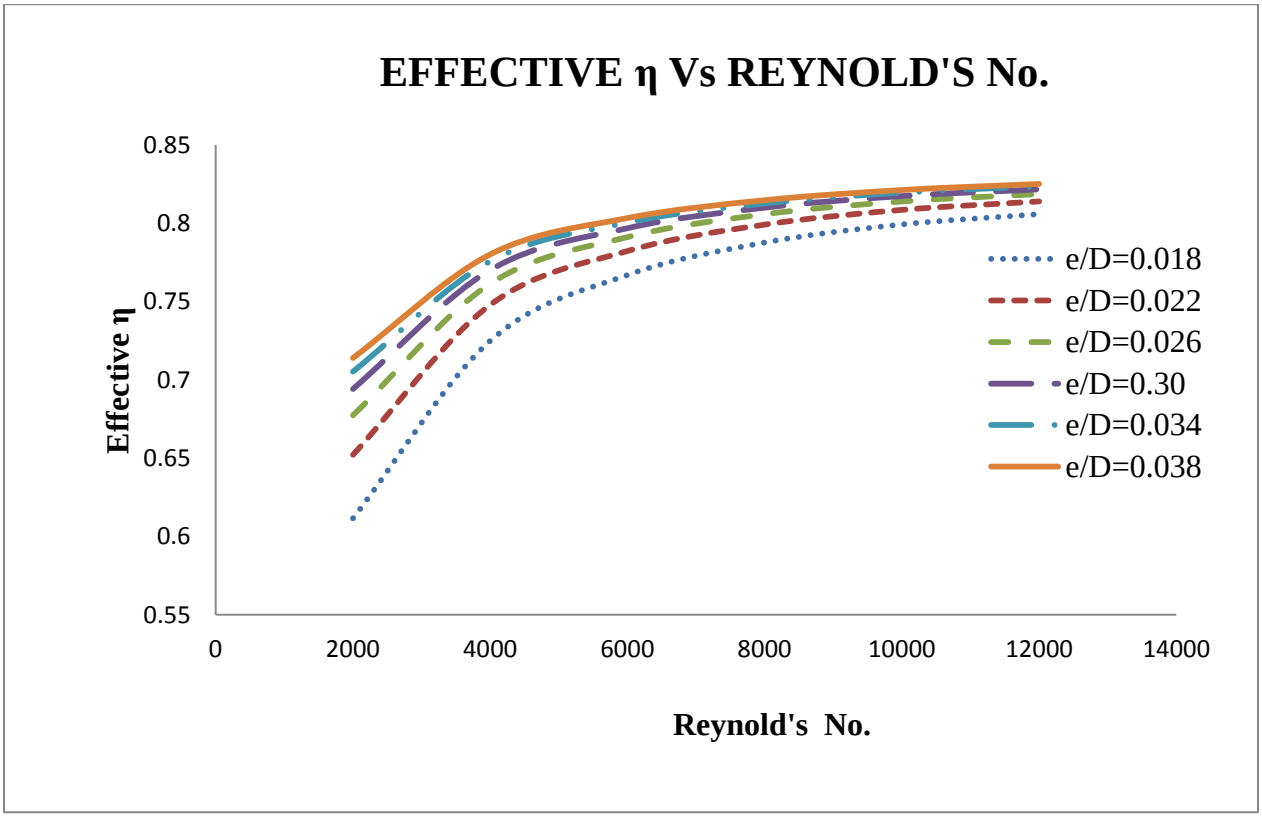

Figure 4.4 Variation of Effective Efficiency with Reynolds's No. (Dimple Shaped Ribs)

From the figure 4.4 it is clear that effective efficiency increases continuously with Reynolds's number for all relative roughness height (e/D) and attains corresponding maximum values. In this case value of relative roughness pitch (p/e) is 12 for all the relative roughness height (e/D). It was also found that effective efficiency attains a maximum value of approx. 0.8251 at Reynolds's no. of 12000 for relative roughness height of 0.038.

4.1.5 Effective Efficiency of Solar Air Heater Provided with Metal Grit Ribs

Figure 4.5 shows the variation of effective efficiency w.r.t Reynolds's number for solar air heater provided with metal grit ribs as a roughness element on its absorber plate.

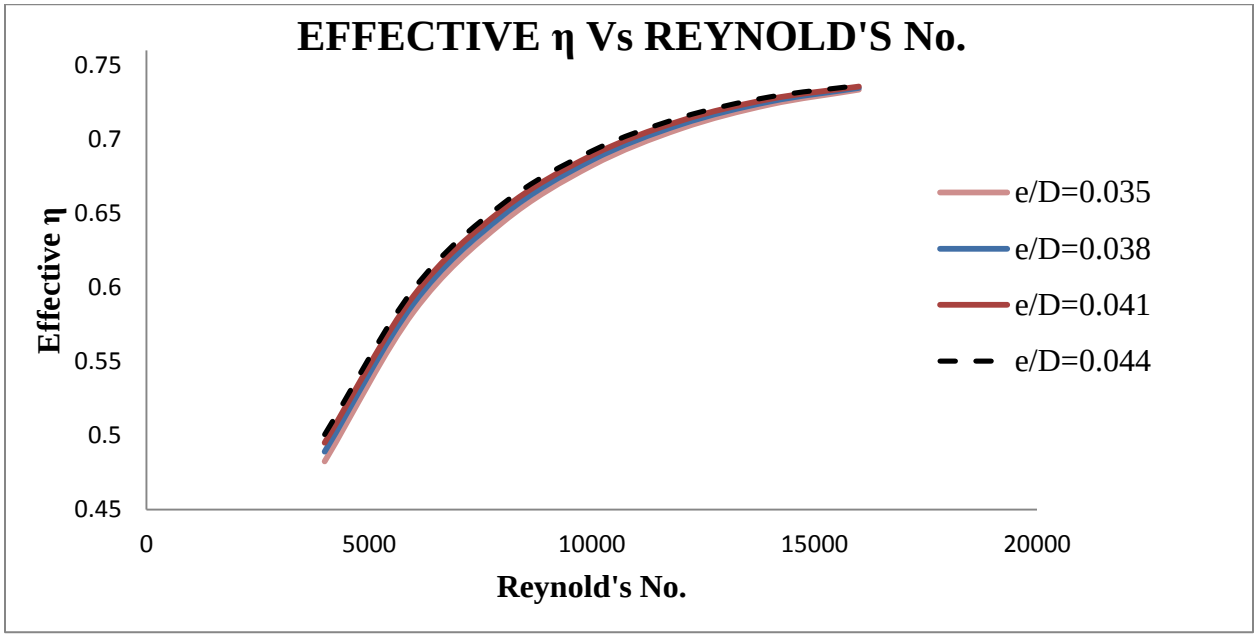

Figure 4.5 Variation of Effective Efficiency with Reynolds's No. (Metal Grit Ribs)

From the figure 4.5 it is clear that effective efficiency increases continuously with Reynolds's number for all relative roughness height (e/D) and attains corresponding maximum values. In this case value of relative roughness pitch (p/e) is 36 for all the relative roughness height (e/D). It was also found that effective efficiency attains a maximum value of approx. 0.7362 at Reynolds's no. of 16000 for relative roughness height of 0.044.

4.1.6 Effective Efficiency of Solar Air Heater Provided with U Shaped Turbulators

Figure 4.6 shows the variation of effective efficiency w.r.t Reynolds's number for solar air heater provided with U shaped Turbulators as a roughness element on its absorber plate.

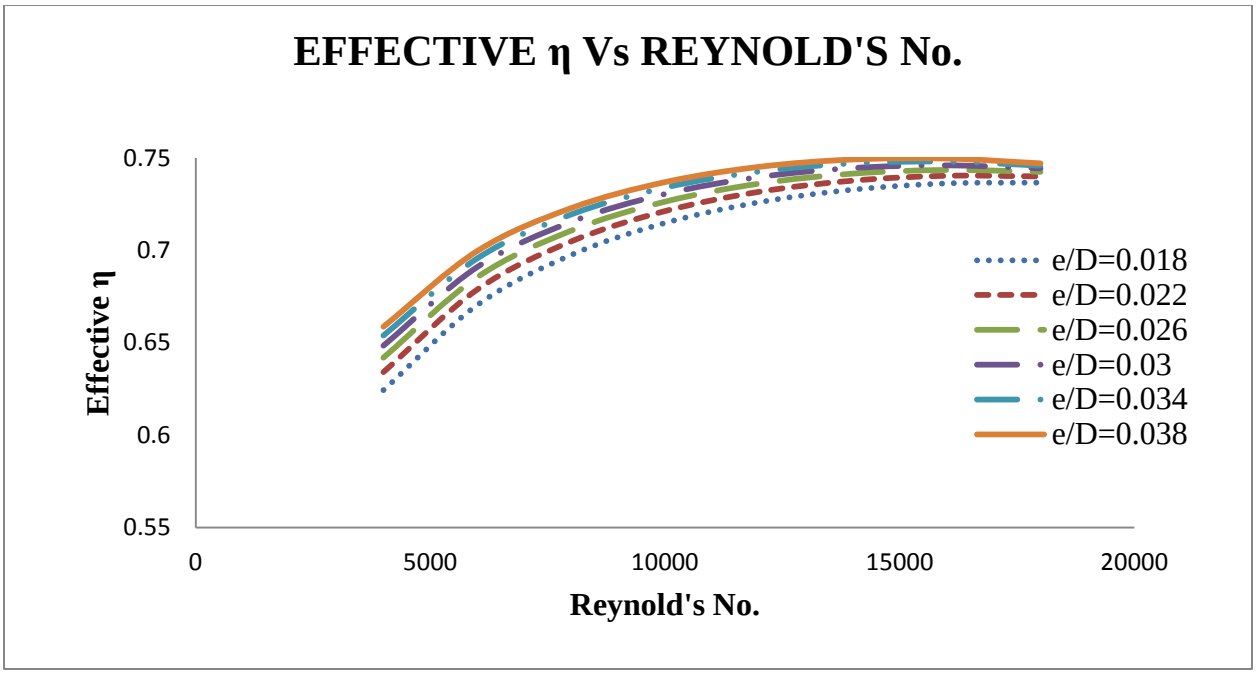

Figure 4.6 Variation of Effective Efficiency with Reynolds's No. (U Shaped Turbulators)

From the figure 4.6 it is clear that effective efficiency increases continuously with Reynolds's number for relative roughness height (e/D) of 0.018 but for all other relative roughness height (e/D) effective efficiency increases continuously up to Reynolds's number 16000 and after that it start decreasing slightly for higher values of Reynolds's number. In this case value of relative roughness pitch (p/e) is 57.14 for all the relative roughness height (e/D). It was also found that effective efficiency attains a maximum value of approx. 0.7396 at Reynolds's no. of 16000 for relative roughness height of 0.038.

4.1.7 Effective Efficiency of Solar Air Heater Provided with Combination of Inclined and Transverse Ribs

Figure 4.7 shows the variation of effective efficiency w.r.t Reynolds's number for solar air heater provided with combination of inclined and transverse ribs as a roughness element on its absorber plate.

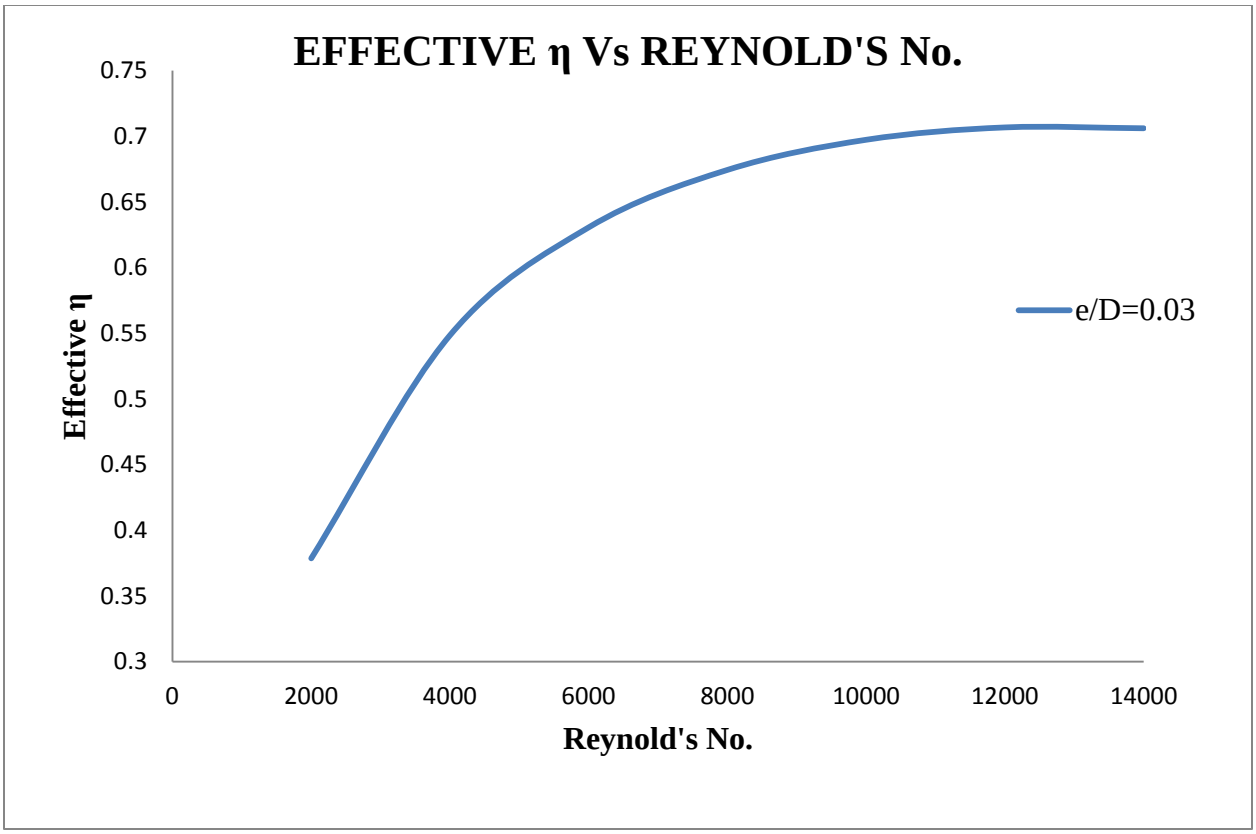

Figure 4.7 Variation of Effective Efficiency with Reynolds's No. (Inclined and Transverse Ribs)

From the figure 4.7 it is clear that effective efficiency increases continuously up to Reynolds's number 12000 for relative roughness height (e/D) of 0.03 but after that it start decreasing slightly for greater value of Reynolds's number. In this case value of relative roughness pitch (p/e) is 8. It was also found that effective efficiency attains a maximum value of approx. 0.7067 at Reynolds's no. of 12000 for relative roughness height of 0.03.

4.1.8 Effective Efficiency of Solar Air Heater Provided with Arc Shaped Wire

Figure 4.8 shows the variation of effective efficiency w.r.t Reynolds's number for solar air heater provided with arc shaped wire as a roughness element on its absorber plate.

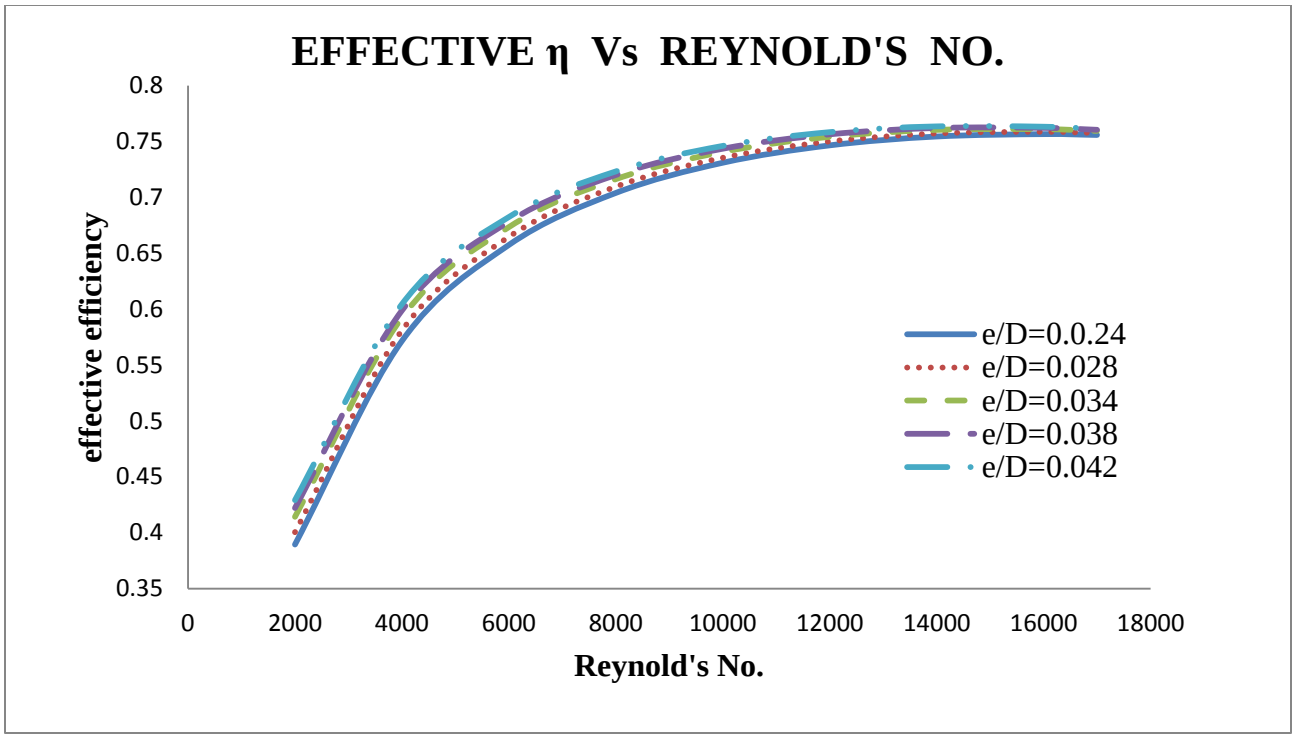

Figure 4.8 Variation of Effective Efficiency with Reynolds's No. (Arc Shaped Wire)

From the figure 4.8 it is clear that effective efficiency increases continuously up to Reynolds's number 16000 for all relative roughness height (e/D) and attains corresponding maximum values and after that it starts decreasing slightly for higher value of Reynolds's number. In this case value of relative roughness pitch (p/e) is 10 for all the relative roughness height (e/D). It was also found that effective efficiency attains a maximum value of approx. 0.7631 at Reynolds's no. of 16000 for relative roughness height of 0.042.

4.1.9 Comparison of Effective Efficiencies for Different Solar Air Heaters

Figure 4.9 shows the variation of effective efficiency w.r.t Reynolds's number for solar air heaters provided with different roughness geometries on its absorber plate by keeping the value of relative roughness height (e/D) 0.034

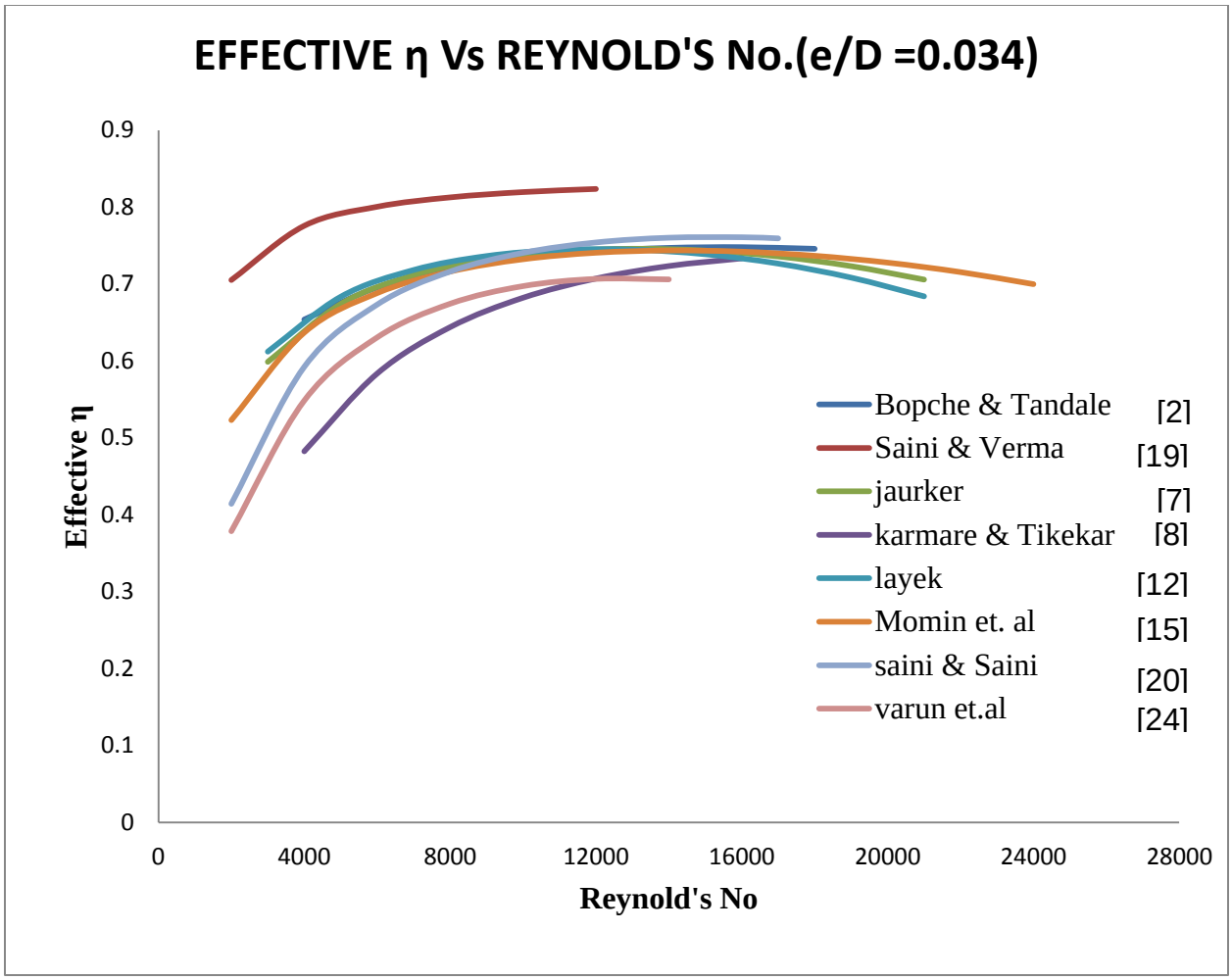

Figure 4.9 Variation of Effective Efficiency with Reynolds's No.
(Different Roughened Solar Air Heaters)

From the figure 4.9 it is clear that in the lower range of Reynolds's number(less than 12000) Dimple shaped ribs resulted in better effective efficiency. However in higher range of Reynolds's number (greater than 12000) Arc shaped wires resulted in better effective efficiency. It was also found that under present study effective efficiency attains a maximum value for dimple shaped ribs of approx. 0.8236 at Reynolds's no. of 12000 for relative roughness height of 0.034.

4.2 SIMULATION RESULTS

In present work following the simulation methodology and utilizing the boundary conditions as mentioned in detail in Chapter 3, simulations were completed to obtain following results

1. Temperature distribution in roughened solar air heater.
2. Velocity distribution in roughened solar air heater.
3. Flow behaviour of air inside the solar air heater

4.2.1 Simulation Results of Solar Air Heater Roughened with V Shaped Ribs

4.2.1.1 Temperature Distribution

From the temperature distribution plot of the system as shown in figure 4.10 and 4.11, atmospheric air enters the solar air heater at 27°C and leaves at 37°C. This variation in temperature was due to radiative and convective heat transfer from the roughened absorber plate

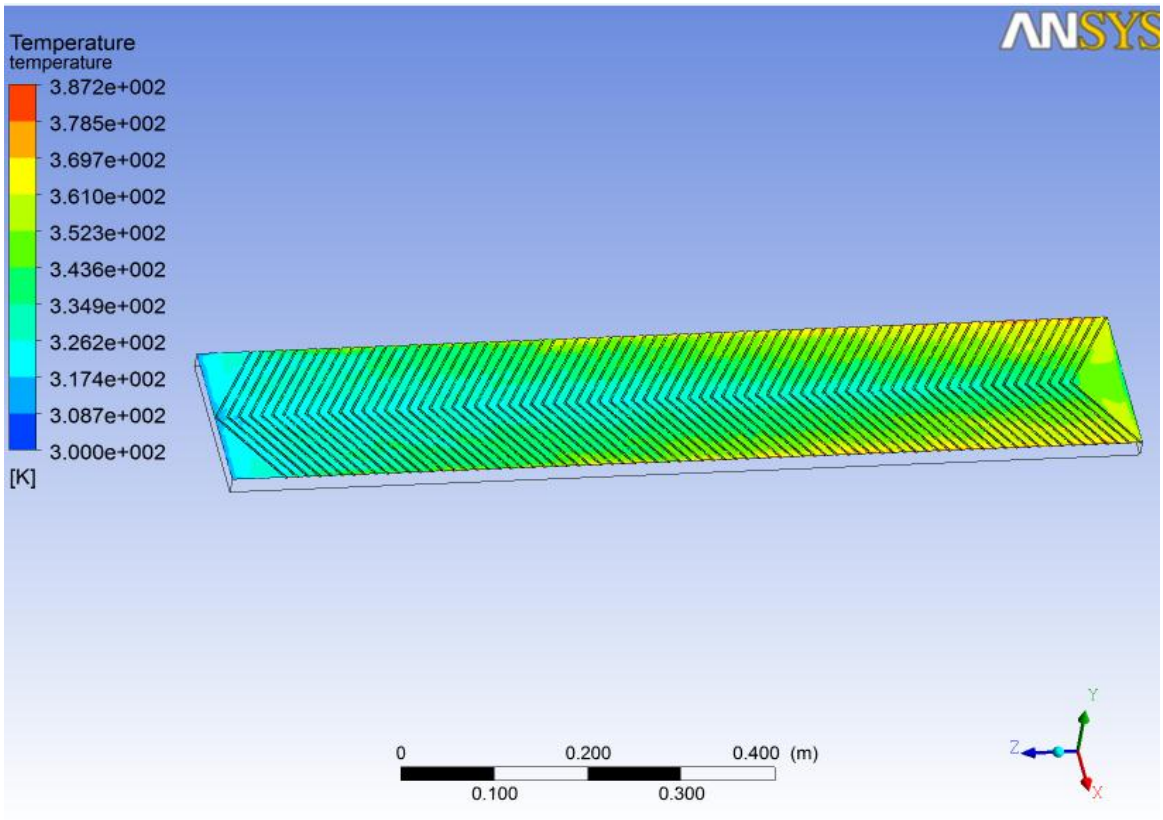

Figure 4.10 Temperature distribution of Air in Solar Air Heater (V Shaped Ribs)

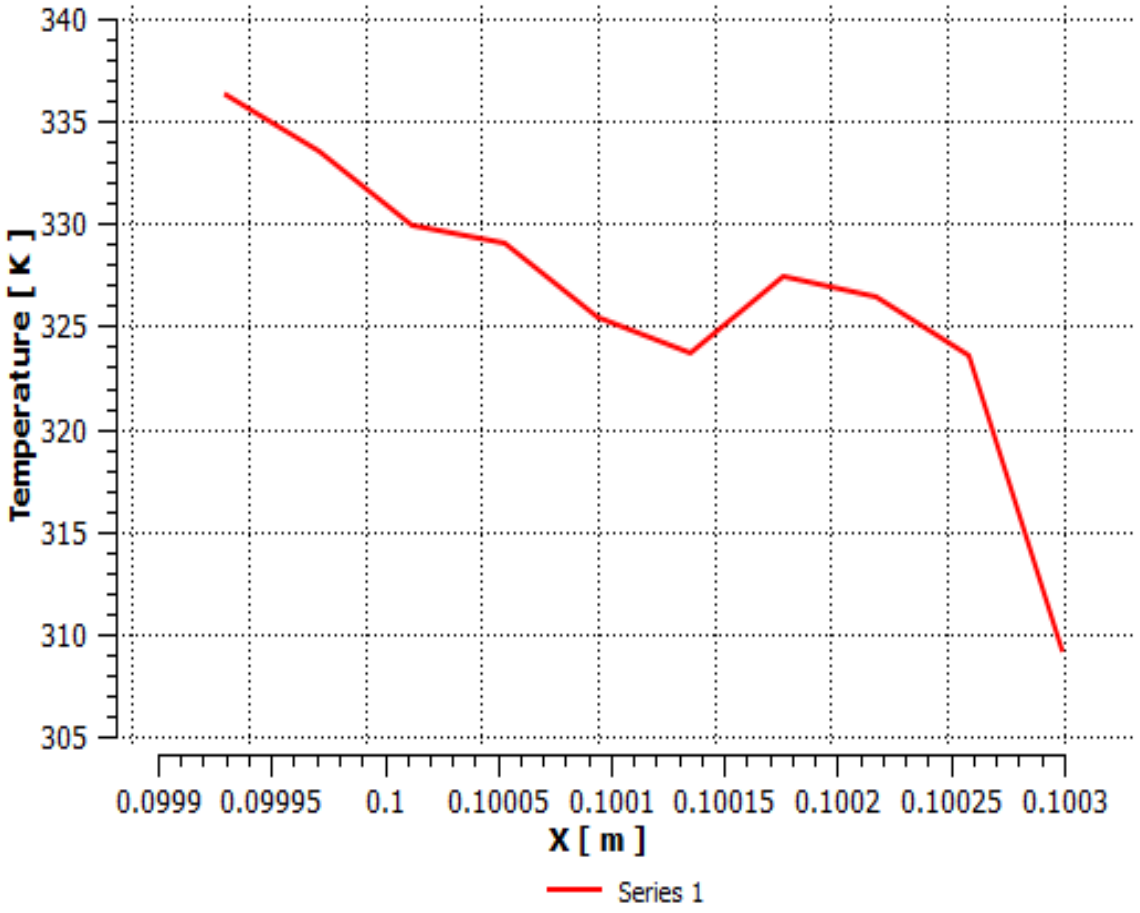

Figure 4.11 Temperature Plot of Air through Solar Air Heater (V Shaped Ribs)

Under the same operating conditions the outlet temperature obtained by numerical analysis is 42°C.

Measured Outlet Temperature	(°C)
CFD Analysis	37
Numerical Analysis	42

Table 4.1 Comparison of Outlet Temperature (V Shaped Ribs)

4.2.1.2 Velocity Distribution

Figure 4.12 shows the velocity distribution inside the solar air heater provided with V shaped roughness.

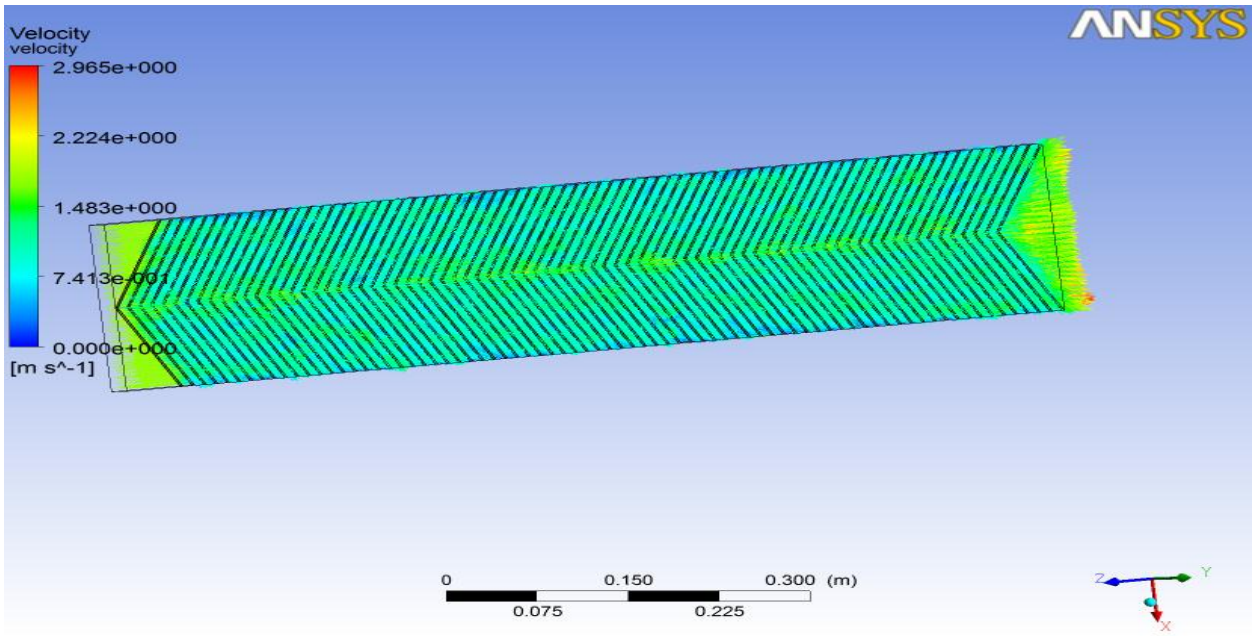

Figure 4.12 Velocity Distribution (V Shaped Ribs)

4.2.1.3 Velocity Streamline

It was observed that air flow velocity in the solar air heater is uniform as shown in figure 4.13 with an outlet velocity of 1.76m/s

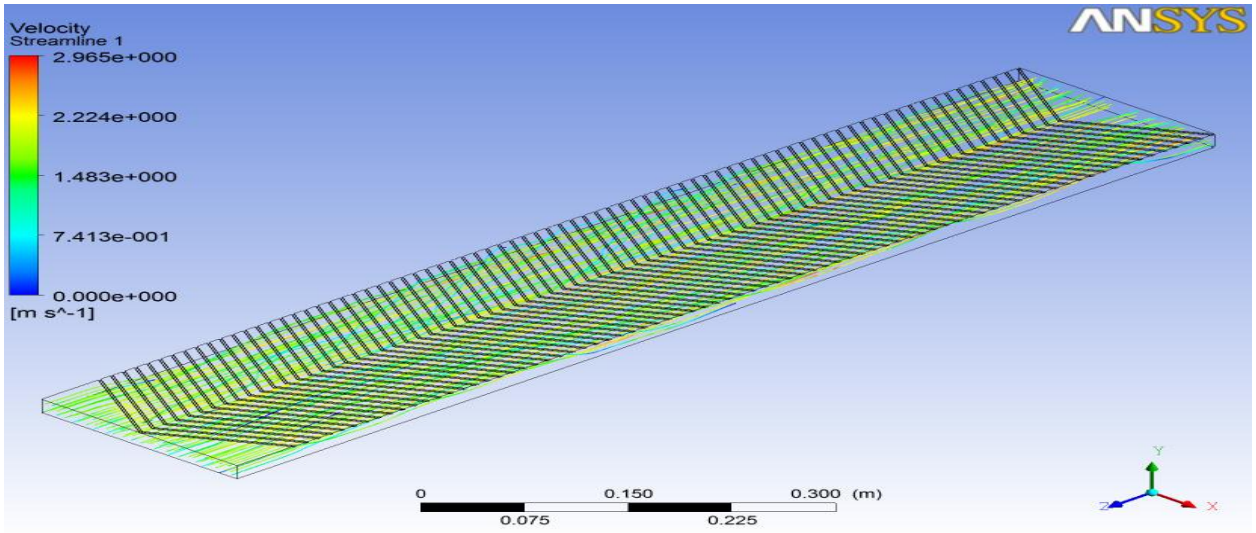

Figure 4.13 Streamline Pattern (V Shaped Ribs)

4.2.2 Simulation Results of Solar Air Heater Roughened with Grooved Ribs

4.2.2.1 Temperature Distribution

From the temperature distribution plot of the system as shown in figure 4.14 and 4.15, atmospheric air enters the solar air heater at 27°C and leaves at 67°C.

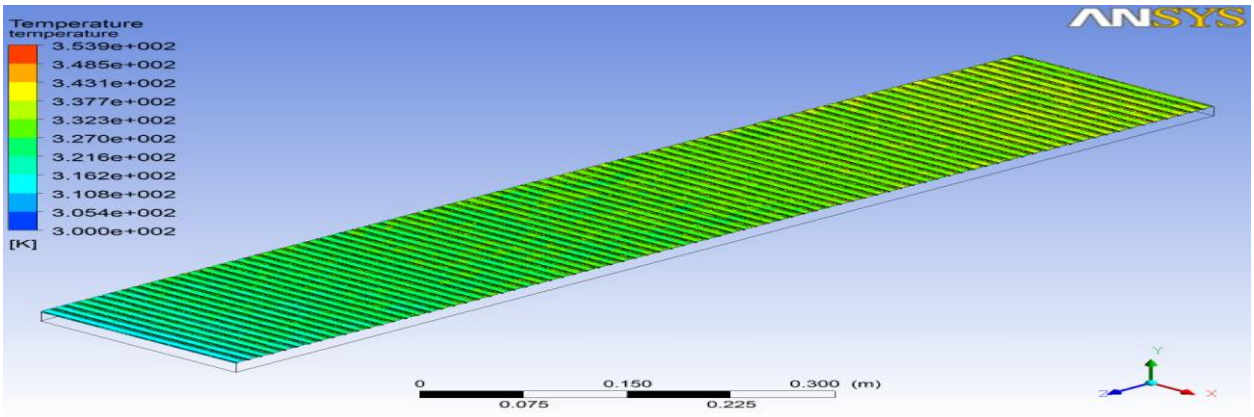

Figure 4.14 Temperature distribution of Air in Solar Air Heater (Grooved Ribs)

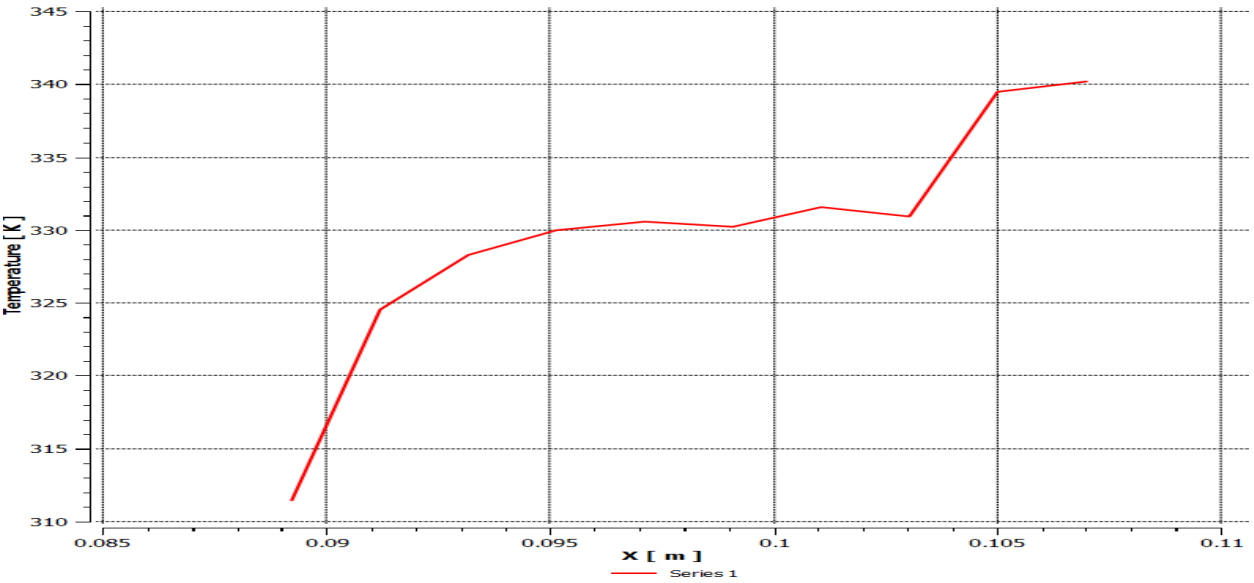

Figure 4.15 Temperature Plot of Air through Solar Air Heater (Grooved Ribs)

Under the same operating conditions the outlet temperature obtained by numerical analysis was 65°C.

Measured Outlet Temperature	(°C)
CFD Analysis	67
Numerical Analysis	65

Table 4.2 Comparison of Outlet Temperature (Grooved Ribs)

4.2.2.2 Velocity Distribution

Figure 4.16 shows the velocity distribution inside the solar air heater provided with Grooved ribs.

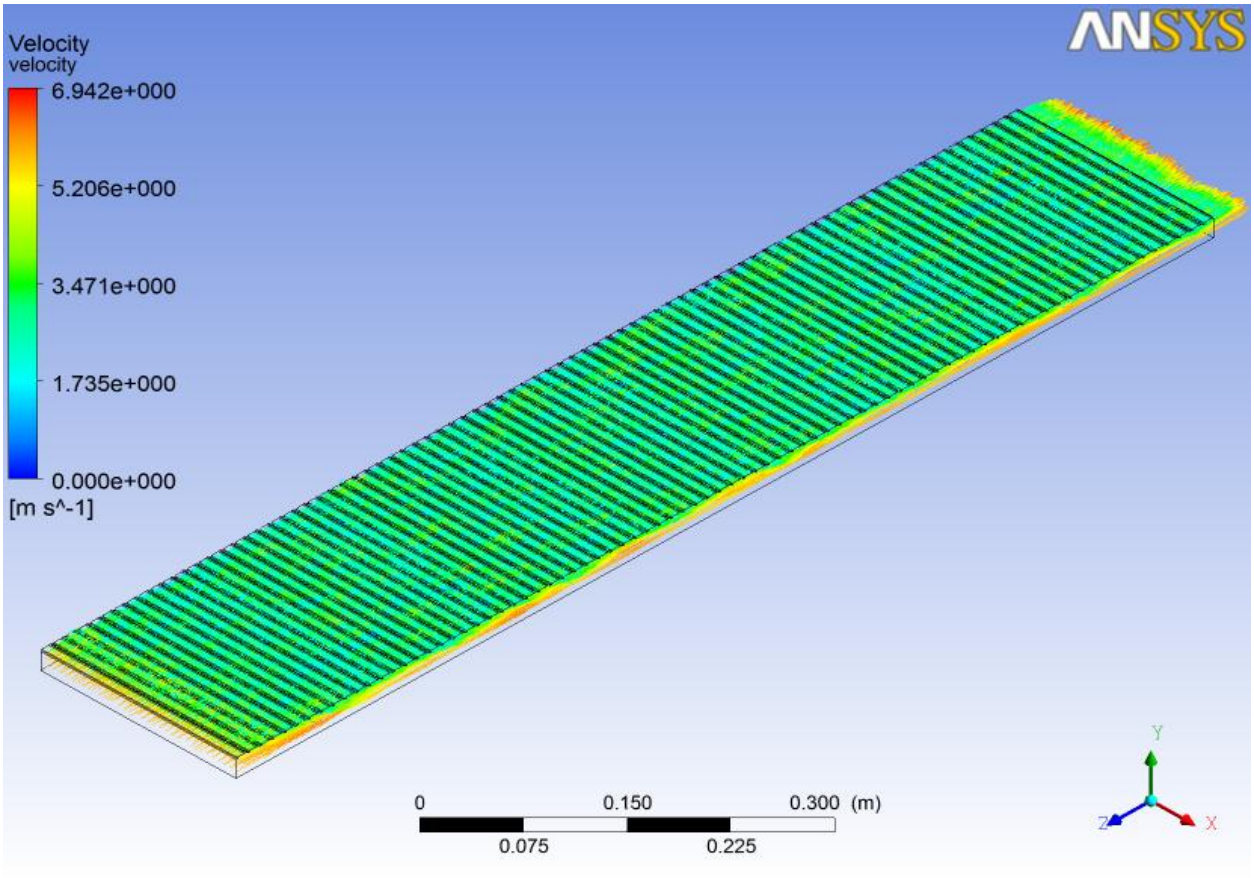

Figure 4.16 Velocity Distribution (Grooved Ribs)

4.2.2.3 Velocity Streamline

It was observed that air flow velocity in the solar air heater is uniform as shown in figure 4.17 with an outlet velocity of 5.72m/s

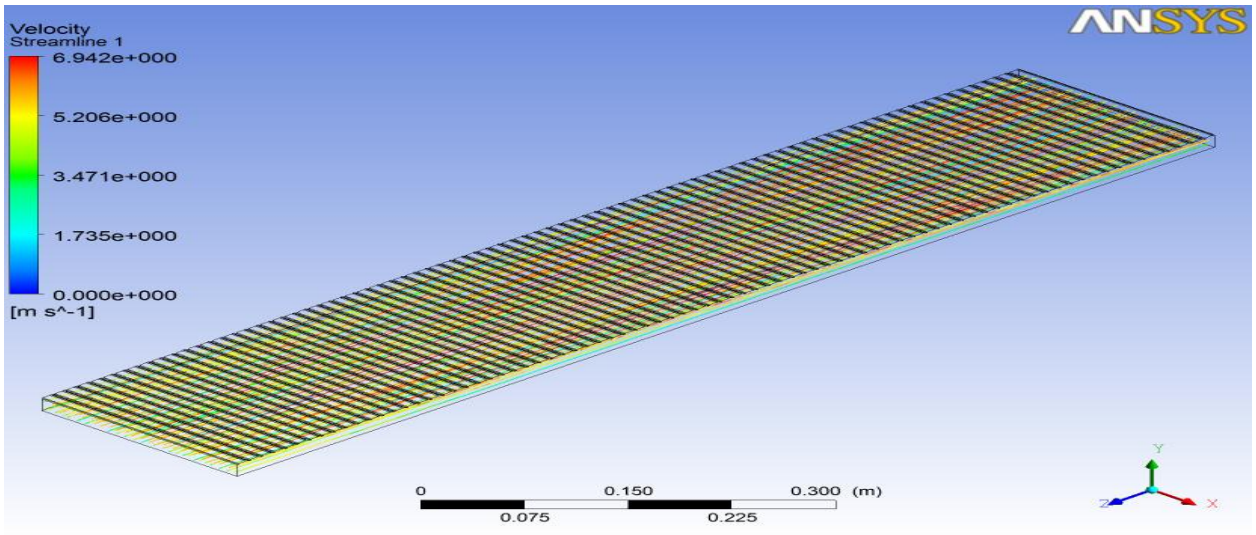

Figure 4.17 Streamline Pattern (Grooved Ribs)

4.2.3 Simulation Results of Solar Air Heater Roughened with Chamfered Grooved Ribs

4.2.3.1 Temperature Distribution

From the temperature distribution plot of the system as shown in figure 4.18 and 4.19, atmospheric air enters the solar air heater at 27°C and leaves at 38°C.

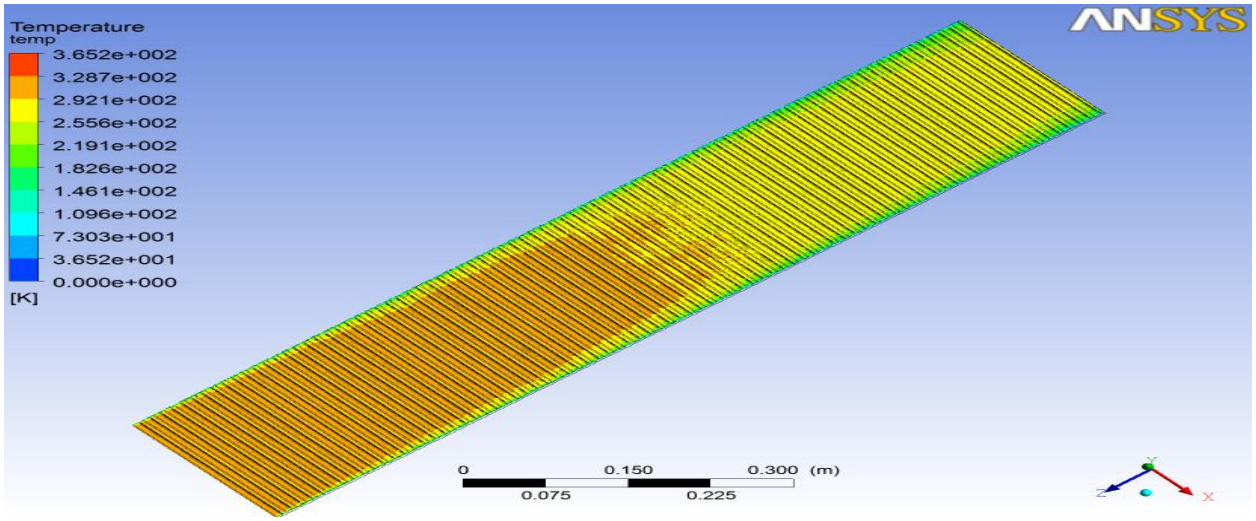

Figure 4.18 Temperature distribution of Air in Solar Air Heater (Chamfered Grooved Ribs)

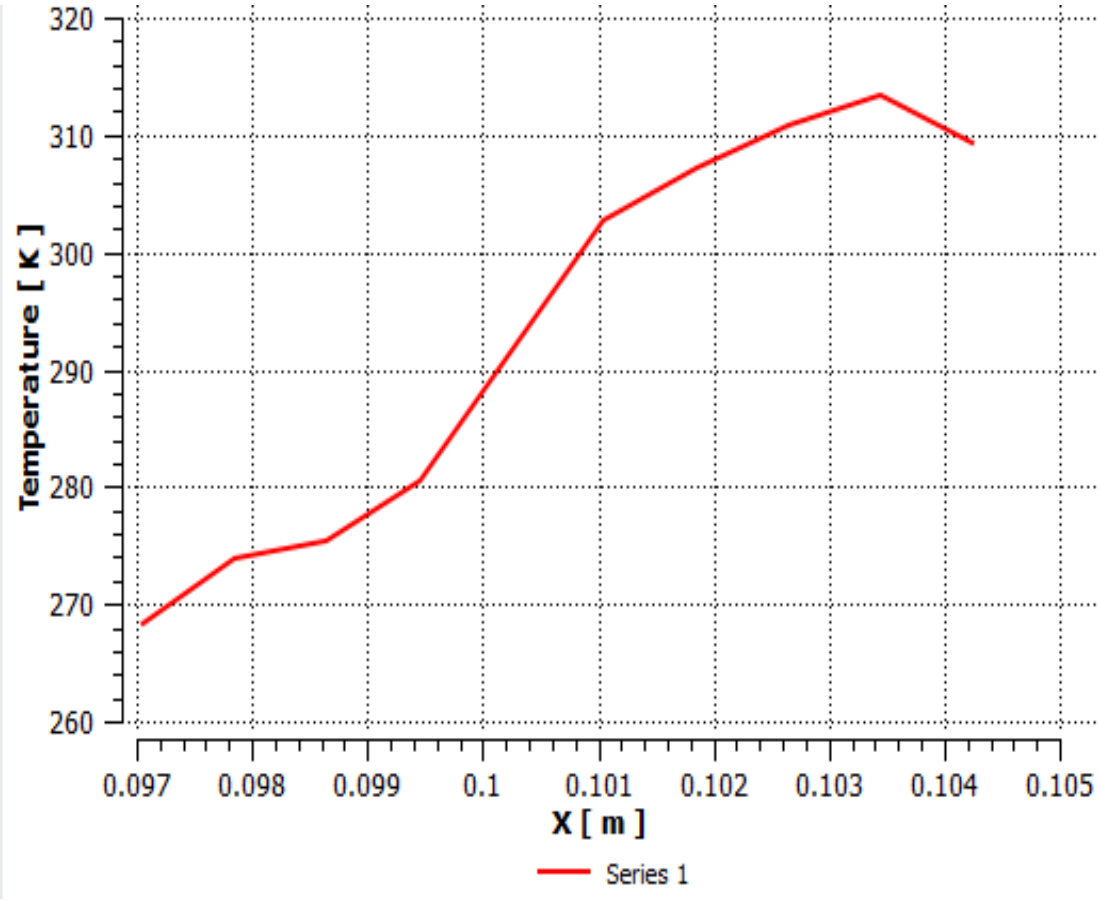

Figure 4.19 Temperature Plot of Air through Solar Air Heater (Chamfered Grooved Ribs)

Under the same operating conditions the outlet temperature obtained by numerical analysis was 33°C.

Measured Outlet Temperature	(°C)
CFD Analysis	38
Numerical Analysis	33

Table 4.3 Comparison of Outlet Temperature (Chamfered Grooved Ribs)

4.2.3.2 Velocity Distribution

Figure 4.20 shows the velocity distribution inside the solar air heater provided with Chamfered Grooved ribs.

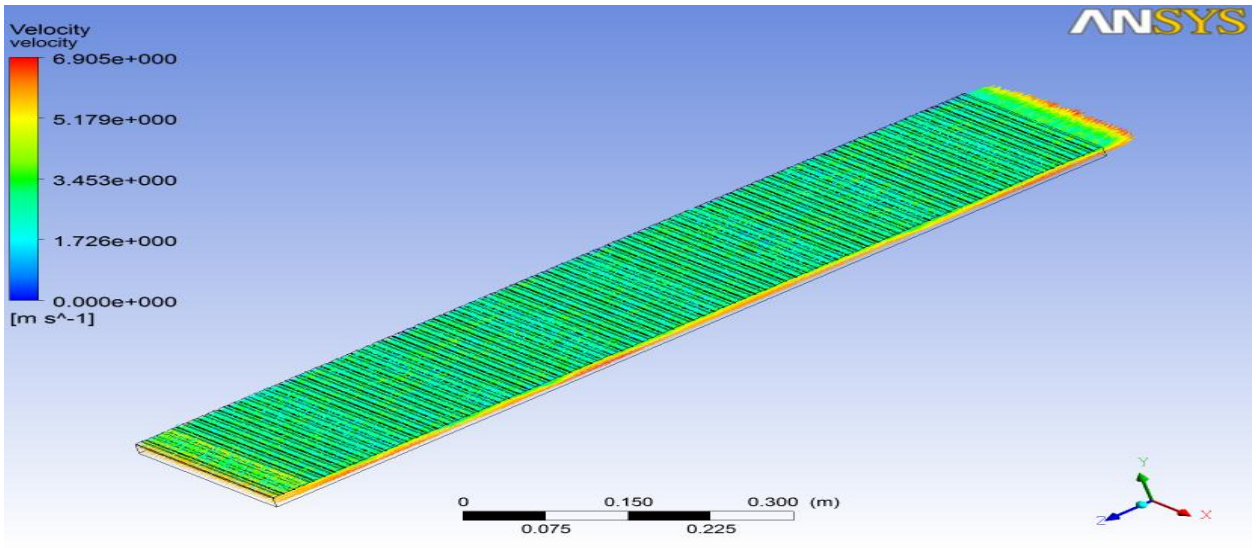

Figure 4.20 Velocity Distribution (Chamfered Grooved Ribs)

4.2.3.3 Velocity Streamline

It was observed that air flow velocity in the solar air heater is uniform as shown in figure 4.21 with an outlet velocity of 5.72m/s

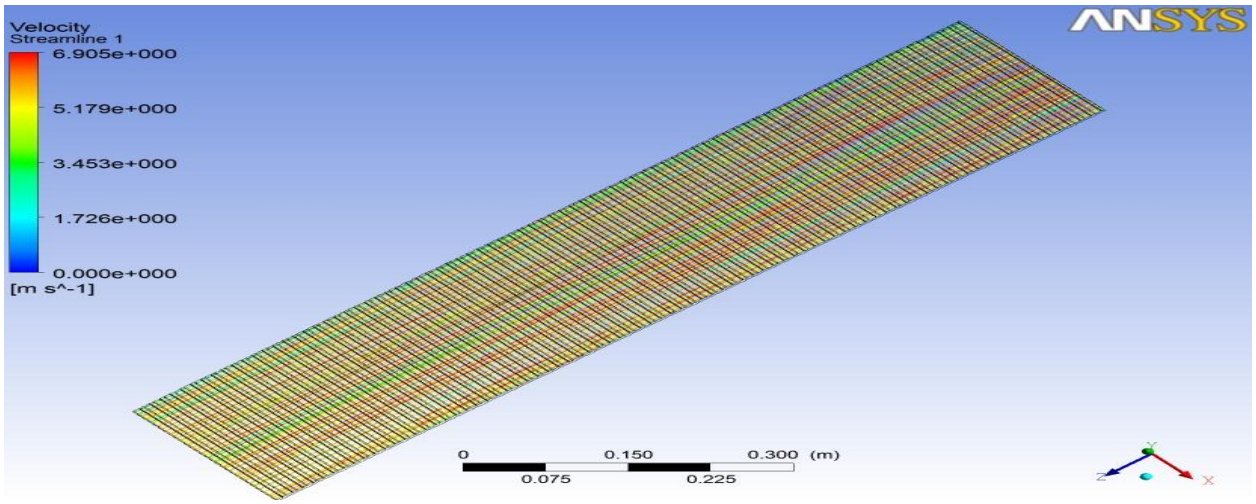

Figure 4.21 Streamline Pattern (Chamfered Grooved Ribs)

4.2.4 Simulation Results of Solar Air Heater Roughened with Dimple Shaped Ribs

4.2.4.1 Temperature Distribution

From the temperature distribution plot of the system as shown in figure 4.22 and 4.23, atmospheric air enters the solar air heater at 27°C and leaves at 51°C.

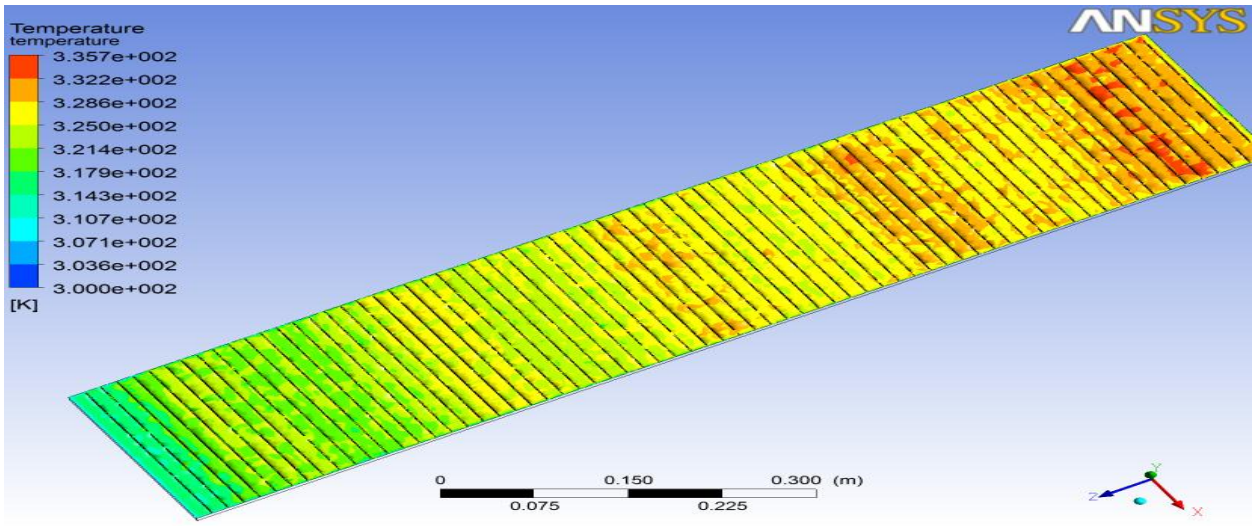

Figure 4.22 Temperature distribution of Air in Solar Air Heater (Dimple Shaped Ribs)

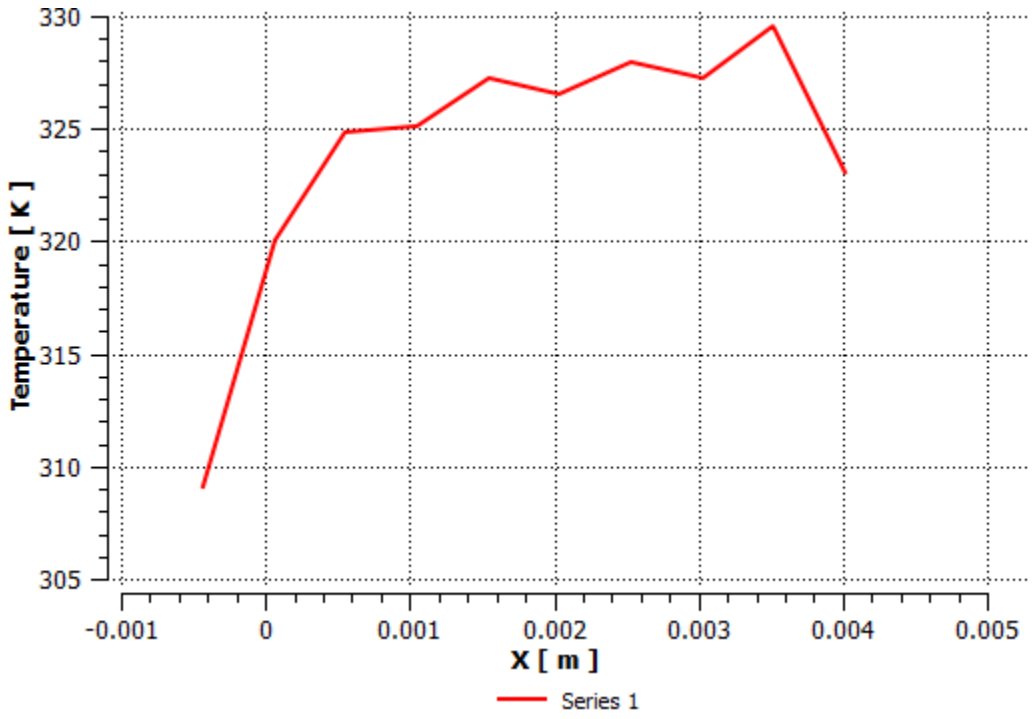

Figure 4.23 Temperature Plot of Air through Solar Air Heater (Dimple Shaped Ribs)

Under the same operating conditions the outlet temperature obtained by numerical analysis was 46°C.

Measured Outlet Temperature	(°C)
CFD Analysis	51
Numerical Analysis	46

Table 4.4 Comparison of Outlet Temperature (Dimple Shaped Ribs)

4.2.4.2 Velocity Distribution

Figure 4.24 shows the velocity distribution inside the solar air heater provided with Dimple shaped ribs.

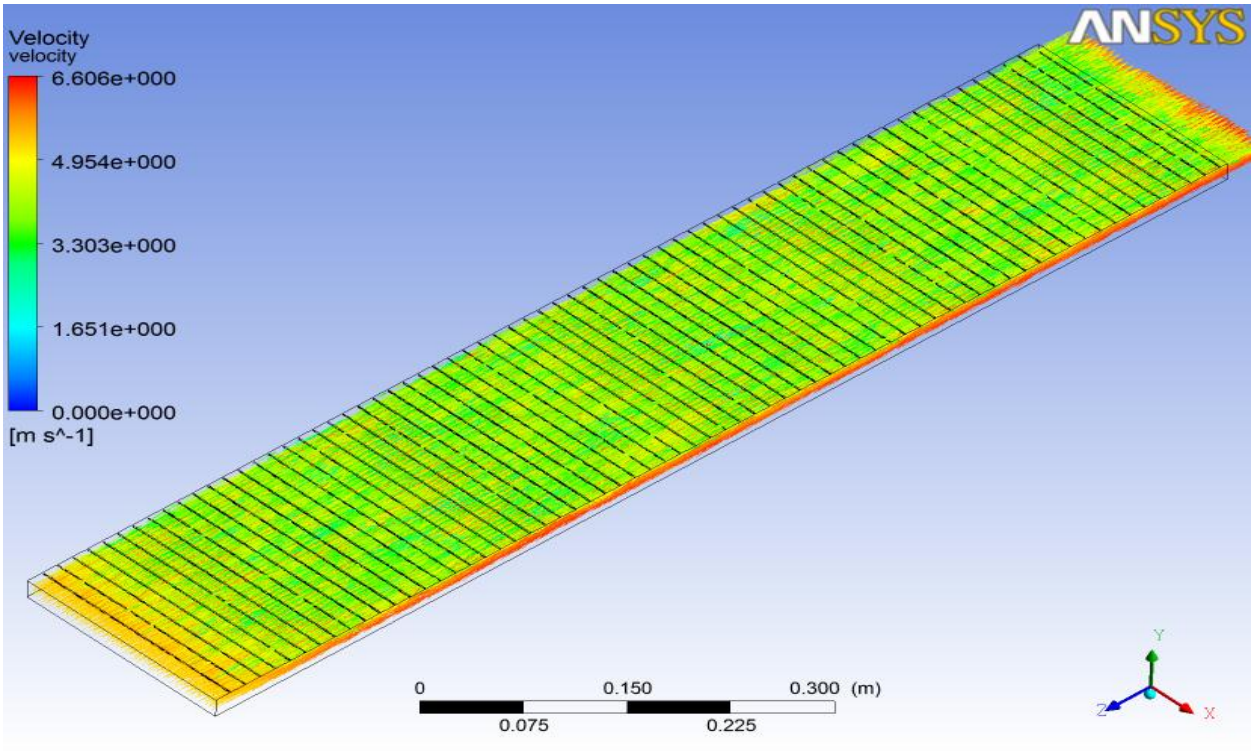

Figure 4.24 Velocity Distribution (Dimple Shaped Ribs)

4.2.4.3 Velocity Streamline

It was observed that air flow velocity in the solar air heater is uniform as shown in figure 4.25 with an outlet velocity of 5.28m/s

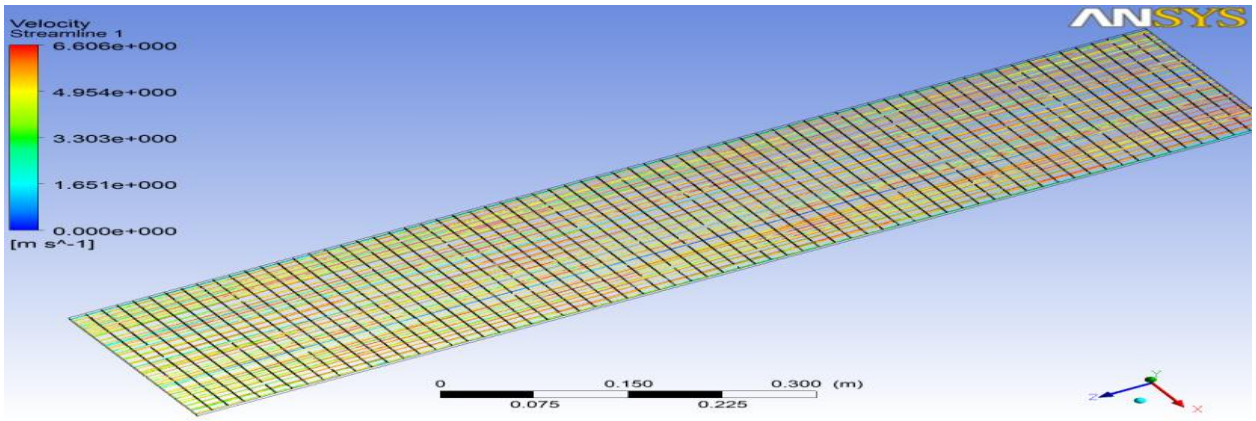

Figure 4.25 Streamline Pattern (Dimple Shaped Ribs)

4.2.5 Simulation Results of Solar Air Heater Roughened with U Shaped Turbulators

4.2.5.1 Temperature Distribution

From the temperature distribution plot of the system as shown in figure 4.26 and 4.27, atmospheric air enters the solar air heater at 27°C and leaves at 49°C

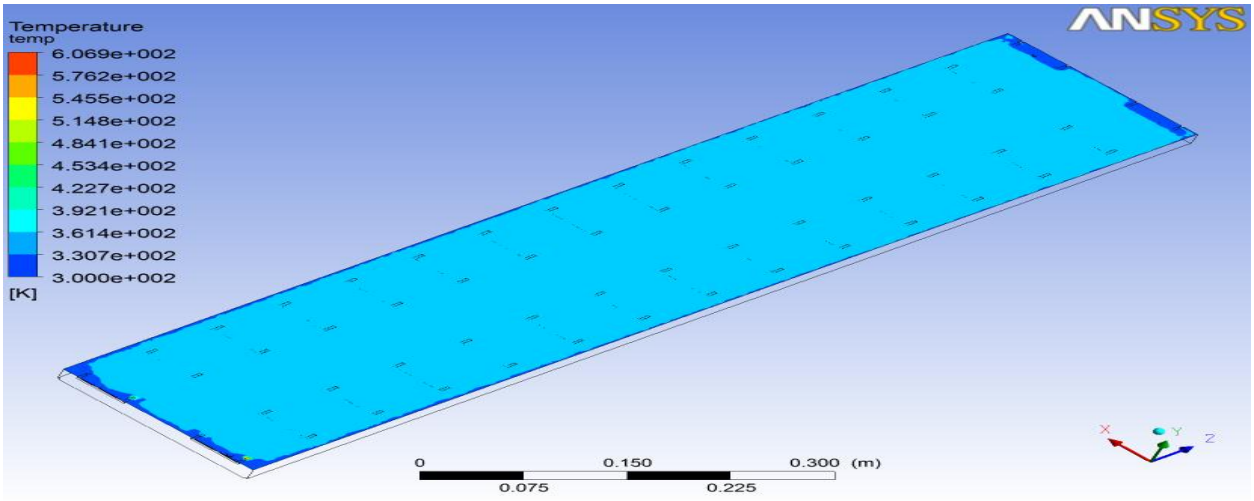

Figure 4.26 Temperature distribution of Air in Solar Air Heater (U Shaped Turbulators)

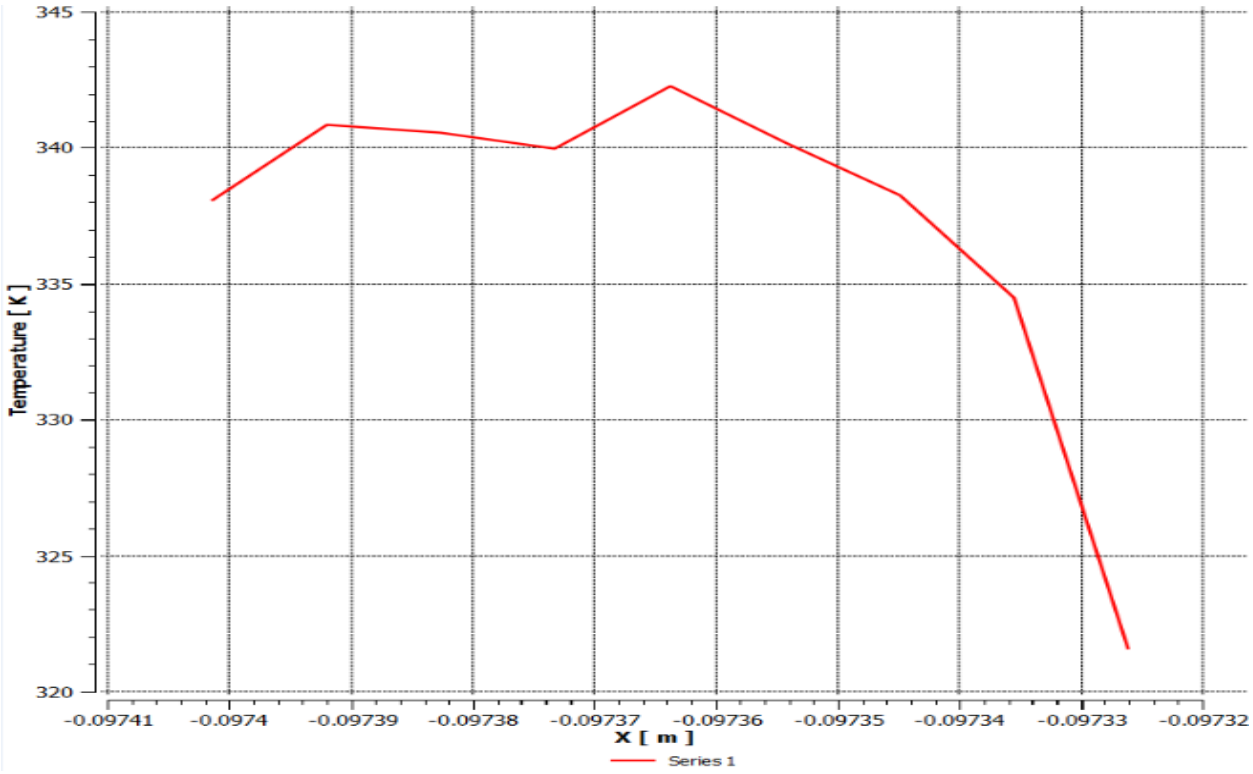

Figure 4.27 Temperature Plot of Air through Solar Air Heater (U Shaped Turbulators)

Under the same operating conditions the outlet temperature obtained by numerical analysis was 43°C.

Measured Outlet Temperature	(°C)
CFD Analysis	49
Numerical Analysis	43

Table 4.4 Comparison of Outlet Temperature (U Shaped Turbulators)

4.2.5.2 Velocity Distribution

Figure 4.28 shows the velocity distribution inside the solar air heater provided with U shaped turbulators.

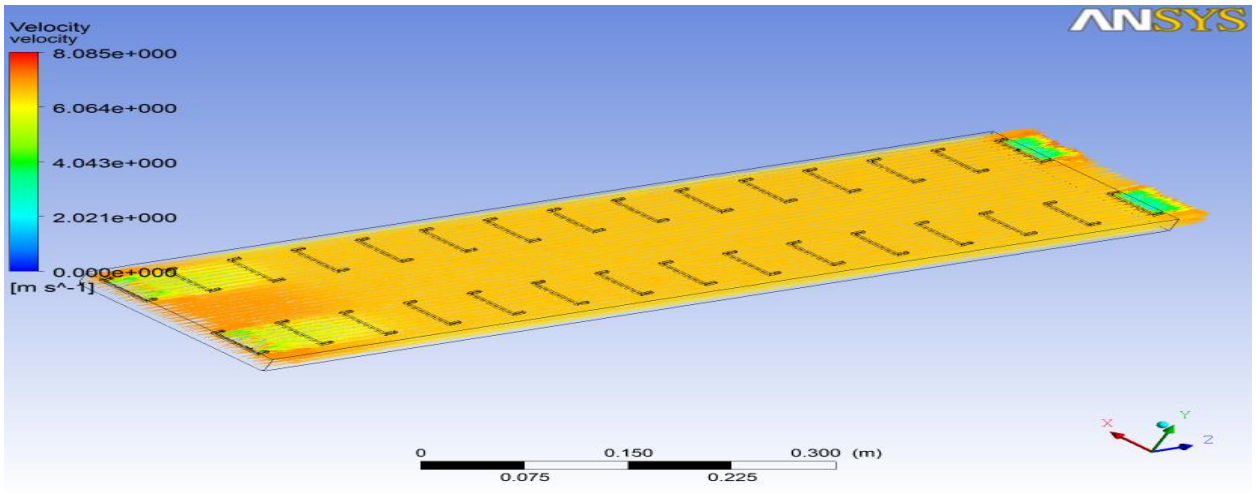

Figure 4.28 Velocity Distributions (U Shaped Turbulators)

4.2.5.3 Velocity Streamline

It was observed that air flow velocity in the solar air heater is uniform as shown in figure 4.29 with an outlet velocity of 7.04m/s

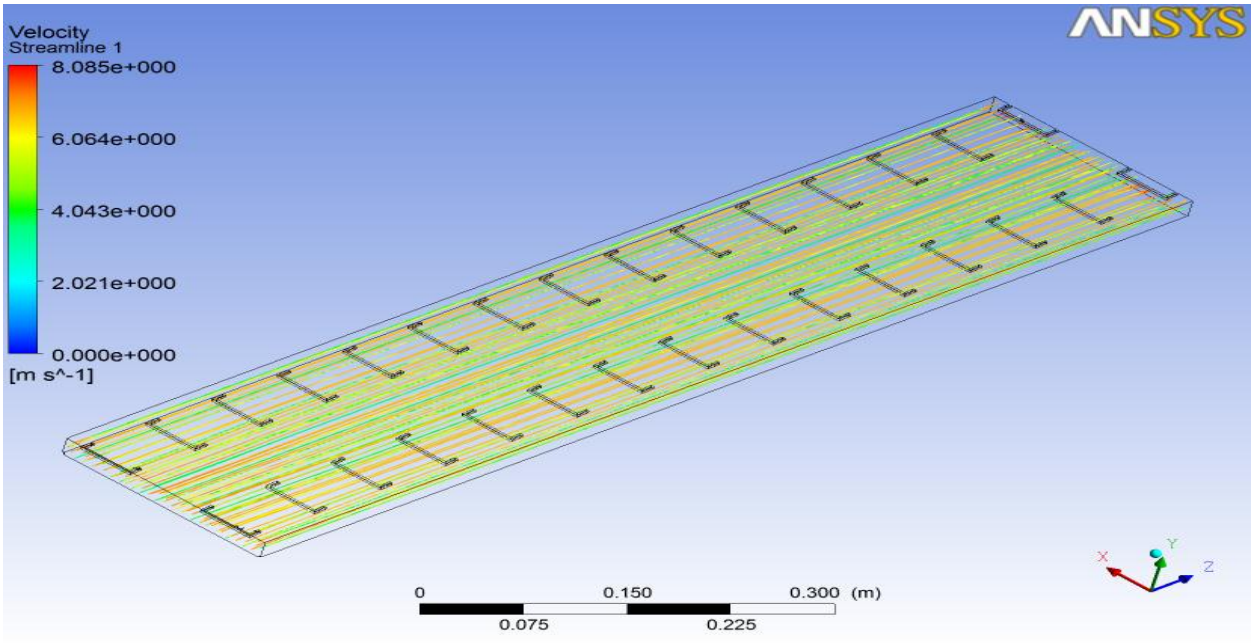

Figure 4.29 Streamline Pattern (U Shaped Turbulators)

CHAPTER 5
CONCLUSION AND FUTURE SCOPE

5.1 CONCLUSION

Present work is done to analyze the performance of artificially roughened solar air heaters solar in terms of effective efficiency. First of all mathematical modelling is done to theoretically predict the performance of artificially roughened solar air heaters. The solar air heater is modeled by using heat energy balance equation which governs the solar air heater performance. Secondly using the Fluid flow (FLUENT) module of ANSYS heat transfer analysis was conducted on the solar air heaters. The main aim of this analysis is to solve the heat transfer that take place from absorber plate to moving air in the solar air heater. This simulation module predicts the velocity and outlet temperature of the air.

Based on the results of the present work, following conclusions were drawn:

1 There is a significant improvement in effective efficiency of solar air heater by providing different types of roughness elements on t he absorber plate.

2 In the lower range of Reynolds's number(less than 12000) Dimple shaped ribs resulted in better effective efficiency. However in higher range of Reynolds's number (greater than 12000) Arc shaped wire resulted in better thermal efficiency.

3 Under present study effective efficiency attains a maximum value for dimple shaped ribs of approx. 0.8236 at Reynolds's no. of 12000 for relative roughness height of 0.034.

4 Under present study solar air heater provided with grooved ribs on its absorber plate give maximum enhancement in outlet temperature of air.

5.2 FUTURE SCOPE

1 In present work few roughness geometries are under investigation. So further performance analysis can be done using various other roughness geometries.

2 In present work for all the roughness geometries under investigation effective efficiency is calculated by varying the relative roughness height (e/D) while kept the other operating parameters constant. So there is a large scope for predicting the performance in terms of

effective efficiency by varying the other operating parameters such as relative roughness pitch(p/e).

3 In present work simulation is carried out to predict the flow behaviour along the length of roughened solar air heater but actually there is also a variation in flow behaviour along the height of air passage that can be included in further studies.

REFERENCES

[1] Aloyem Kaze Claude V, Rene Tchinda, "On the Comparison of Some Selected Artificial Roughness Geometries Used in Solar Air Collectors", Exergy and Energy Analysis, 2010, vol. 45, no.2, pp. 232-248.

[2] Bopche S.B., Tandale M.S., "Experimental Investigation on Heat Transfer and Friction Characteristics of a Turbulator Roughened Solar Air Heater Duct", International Journal of Heat and Mass Transfer, 2009, vol.52, pp.2834-2848.

[3] Chaube Alok, Sahoo P.K., Solanki S.C., "Analysis of Heat Transfer Augmentation and Flow Characteristics Due to Rib Roughness Over Absorber Plate of a Solar Air Heater", Renewable Energy, 2006, vol.31, pp.317-331.

[4] Cortes A, Piacentini R, "Improvement of the Efficiency of a Bare Solar Collector by Means of Turbulence Promoters", Applied Energy, 1990, vol.36, pp.253–6.

[5] Gupta D., Solanki S.C., Saini J.S., "Heat and Fluid Flow in Rectangular Solar Air Heater Duct Having Transverse Rib Roughness on Absorber Plate", Solar Energy, 1993, vol.51, pp.31-37.

[6] Gupta D, Solanki S.C., Saini J.S, "Thermo Hydraulic Performance of Solar Air Heaters with Roughened Absorber Plates, Solar Energy, 1997, vol.61, no.1, pp.33–42.

[7] Jaurker A.R., Saini J.S., Gandhi B.K., "Heat Transfer and Friction Characteristics of Rectangular Solar Air Heater Duct Using Rib Grooved Artificial Roughness", Solar Energy, 2006, vol.80, pp.895-907.

[8] Karmare S.V., Tikekar A.N., "Heat Transfer and Friction Factor Correlation for Artificially Roughened Duct with Metal Grit Ribs", International Journal of Heat and Mass Transfer, 2007, vol.50, pp.4342-4351.

[9] Karwa R., Solanki S.C., Saini J.S., "Thermohydraulic Performance of Solar Air Heaters Having Integral Chamfered Rib Roughness on Absorber Plate", Energy, 2001, vol.26, pp161-176.

[10] Kumar S., Saini R.P., "CFD Based Performance Analysis of a Solar Air Heater Duct Provided with Artificial Roughness", Renewable Energy, 2009, vol.34, pp.1285-1291.

[11] Layek Apurba, Saini J.S., Solanki S.C., "Effect of Chamfering on Heat Transfer and Friction Characteristics of Solar Air Heater Having Absorber Plate Roughened with Compound Turbulators", Renewable Energy, 2009, vol.34, pp.1292-1298.

[12] Layek Apurba, Saini J.S., Solanki S.C., "Heat Transfer and Friction Characteristics for Artificially Roughened Duct with Compound Turbulators", International Journal of Heat and Mass Transfer, 2007, vol.50, pp.4845-4854.

[13] Mittal M.K., Varun, Saini R.P., Singal S.K.,"Effective Efficiency of Solar Air Heaters Having Different Types of Roughness Elements On the Absorber Plate", Energy, 2007, vol.32, pp. 739-745.

[14] Mittal M.K., Varun, "Thermo hydraulic Performance of Solar Air Heater Provided with Artificial Roughness on the Absorber Plate", July 2009, vol.90, pp. 43-48.

[15] Momin, Saini J.S., Solanki S.C., "Heat Transfer and Friction in Solar Air Heater Duct with V Shaped Rib Roughness on Absorber Plate", International Journal of Heat and Mass Transfer, 2002, vol.45, pp.3383-3396.

[16] Prasad B.N., Saini J.S., "Effect of Artificial Roughness on Heat Transfer and Friction Factor in a Solar Air Heater", Solar Energy, 1988, vol. 41, no.6, pp. 555.

[17] Rai G.D., "Non Conventional Energy Sources", 4th ed., Khanna Publishers, 2010.

[18] Sahu M.M., Bhagoria J.L., "Augmentation of Heat Transfer Co-Eficient by Using 90° Broken Transverse Rib on Absorber Plate of Solar Air Heater", Renewable Energy, 2005, vol.30, pp.2057-2073.

[19] Saini R.P., Verma J., "Heat Transfer and Friction Correlations for a Duct Having Dimple Shape Artificial Roughness for Solar Air Heater", Energy, 2008, vol.33, pp.1277-1287.

[20] Saini S.K., Saini R.P., "Development of Correlations for Nusselt Number and Friction Factor for Solar Air Heater with Roughened Duct Having Arc Shaped Wire as Artificial Roughness", Solar Energy, 2008, vol.82, pp.1118-1130.

[21] Thakur N.S., Kumar Anoop, Mittal Vijay, "Use of Artificial Roughness to Enhance Heat Transfer in Solar Air Heaters – A Review", Energy, 2010, vol.21, pp.35-51.

[22] Varun, Patnaik Amar, Saini R.P., Singal S.K, Siddhartha, "Performance Prediction of Solar Air Heater Having Roughened Duct Provided with Transverse and Inclined Ribs as Artificial Roughness", Renewable Energy, 2009, vol.34, pp. 2914-2922.

[23] Varun, Saini R.P., Singal S.K., "A Review on Roughness Geometry Used in Solar Air Heaters", Solar Energy, 2007, vol.81, pp. 1340-1350.

[24] Varun, Saini R.P., Singal S.K., "Investigation on Thermal Performance of Solar Air Heaters Having Roughness Elements as a combination of Inclined and Transverse Rib on the Absorber Plate", Renewable Energy, 2008, vol.33, pp.1398-1405.

[25] Verma S.K, Prasad B.N., "Investigation for the Optimal Thermo Hydraulic Performance of Artificially Roughened Solar Air Heaters", Renewable Energy, 2000, vol. 20, pp.19–36.